Experimental Study on Flow Interruption by Cyclopentane Hydrates-in-Water

Robin Jordskar

Thesis for Master of Science Degree at the University of Bergen, Norway

2024

Year: 2024
Title: Experimental Study on Flow Interruption by Cyclopentane Hydrates-in-Water
Author: Robin Jordskar

Acknowledgements

I am deeply grateful for the guidance and support I have received throughout the course of this research. I am immensely grateful for the generous contribution of time, knowledge and resources that has not only made this research possible, but has also enriched my professional and personal development.

Firstly, I would like to express my deepest gratitude to my academic supervisors. Professor Tatyana Kuznetsova has been important in shaping this thesis academically. Her expertise in the field and attention to detail have greatly enhanced both the substance of my research and my skills in academic writing. In addition, professor Boris Balakin from Western Norway University of Applied Sciences has provided invaluable assistance not only in the academic aspects of this study, but also in helping out in the experimental work and analysis of the results. His practical insights and hands-on support have been crucial to the success of the experiments.

Special thanks to Harald Moen and Frode Wessel Jansen from Western Norway University of Applied Sciences, whose practical knowledge and technical skills were essential in the construction and installation of the flow loop used in this research. Their dedication and willingness to help with the practical aspects of this project were indispensable. I am also grateful to Kjetil Gravelsæter, also from Western Norway University of Applied Sciences, for his contributions to the design and construction of essential parts of the flow loop. His expertise in design and construction contributed significantly to the realisation of the experimental set-up.

Finally, I would like to express my heartfelt gratitude to my family and friends for their unwavering support and encouragement throughout my entire academic journey. Their emotional and moral support has been invaluable, not only during the completion of this thesis but throughout all the years of my education. Special thanks go to my grandmother, Hildur, and my mother, Trine, whose support and belief in my abilities have been a continuous source of strength and inspiration.

Abstract

This work investigates the flow behaviour and plugging potential of cyclopentane hydrates within a dynamic flow loop system, focusing on the effects of different hydrate volume fractions. The primary objective was to identify specific hydrate concentrations that significantly affect the hydraulic characteristics of the system and potentially lead to plugging. A custom designed flow loop facilitated a series of experiments to measure pressure drop and identify critical blockage thresholds for hydrate volume fractions ranging from 9.5% to 50%. The study found that blockages typically begin to form at a volume fraction of 40%, with a critical flow rate of approximately 135-140 kg/h, suggesting a specific limit at which the risk of blockage increases significantly. Interestingly, further increases in hydrate concentration did not proportionally increase the severity of plugging, suggesting a potential saturation point in the system's ability to form plugging. The non-cohesive nature of cyclopentane hydrates also highlighted their potential as a less obstructive refrigerant, beneficial for applications such as on-board fish preservation in the fishing industry. The results provide valuable insights into the management of hydrate formation in industrial flow systems and highlight the importance of precise control of hydrate concentration to avoid operational disruptions. Future studies are recommended to further investigate the thermodynamic properties of cyclopentane hydrates, thereby enhancing their application potential in refrigeration and other industrial processes.

Contents

Chapter 1

Introduction

Flow obstruction in oil and gas pipelines due to the accumulation of solids, such as hydrate formation, represents a significant challenge in various industries, including oil and gas production and transportation [1]. Hydrate-induced blockages cause operational difficulties such as potential emergency shutdowns due to their stochastic formation and rapid growth.

These crystalline structures, which are formed when water molecules create cages to encapsulate ”guest” molecules, either from another gas or liquid phase or those already dissolved, represent an innovative approach to refrigeration [2]. Through hydrogen bonding, water molecules arrange themselves around a guest molecule, stabilizing the structure via weak van der Waals forces [1]. Hydrate formation is an exothermic reaction, and dissociation is endothermic. This underscores their potential as a sustainable alternative to conventional refrigerants, which are often harmful to the environment, as hydrate dissociation can be utilized to absorb heat energy from the environment [3].

The fishing industry faces significant challenges in maintaining the freshness and quality of its catch during transport and storage on fishing vessels and factory ships. The enzymatic and bacteriological degradation of fish due to inadequate cooling practices not only reduces the quality of the product but also leads to increased wastage, thereby impacting the economic sustainability of these operations affecting the profitability of large-scale operations [4]. In this context, hydrate slurries, which share many of the properties of ice slurries, have emerged as a promising alternative to traditional cooling methods to address the challenges of fish preservation on fishing vessels and factory ships around the world [2]. To mitigate degradation, the widespread use of synthetic refrigerants in refrigeration systems on board vessels has been identified as a significant contributor to climate and environmental concerns [2]. It is therefore important to investigate alternative, efficient, and economically

viable refrigeration methods that utilise natural refrigerants in order to address these pressing issues effectively. Effective onboard fish preservation through refrigeration not only enhances product quality and shelf life but also reduces food loss [4]. Furthermore, the adoption of refrigeration systems employing natural refrigerants can contribute significantly to reducing fossil fuel consumption and mitigating high-GWP (Global Warming Potential) emissions, thus promoting environmental sustainability in the fishing industry.

The objective of this study is to examine the behavior of cyclopentane hydrates within a flow environment, with a particular focus on their tendency to form plugs. An understanding of the properties of these slurries is essential for the prediction of their flow characteristics and the mitigation of the risks associated with hydrate blockages. Furthermore, an evaluation of the feasibility of cyclopentane hydrates as a practical solution in cooling systems, comparable to the functionality of ice slurry technology, is also of importance.

One of the major advantages of cyclopentane hydrates is that they require less stringent conditions to form. In contrast to ice, which forms only at zero and subzero temperatures, cyclopentane hydrates can form at higher temperatures, thereby reducing the energy intensity of the process. This characteristic significantly reduces the overall energy costs associated with the production and maintenance of hydrates for energy storage applications [5]. The enhanced thermal stability of cyclopentane hydrates makes them particularly practical for storage and transport under varying temperature conditions [6].

Examining the adhesive and cohesive properties of cyclopentane hydrate is a crucial task due to their significant impact on its practical uses, especially within pipeline systems. The adhesive forces between cyclopentane hydrate particles and the surfaces of pipelines or vessels are remarkably low, which minimises the likelihood of hydrates sticking to surfaces and thus reducing the risk of blockages [7]. Furthermore, cyclopentane hydrates exhibit relatively low cohesion between themselves compared to ice, which reduces the likelihood of particles clumping together and forming obstructive plugs that can disrupt fluid flow [8]. The combination of low adhesion and cohesion forces associated with cyclopentane hydrates not only prevent the formation of solid plugs, but also makes them advantageous for use in refrigeration and energy transport systems where maintaining consistent flow and reducing operational challenges are critical.

This study builds upon the groundwork laid by previous research of Struchalin et al.[9, 10, 11, 12], who investigated cohesive particle slurries in a similar flow loop setup. Their findings pertaining to rheological behavior and pressure drop characteristics of ice particle-decane slurries, with a detailed experimental analysis of plug formation and viscosity changes, serve as a

foundational comparison for this work. They discovered flow blockage at a volume fraction of 2.2 to 14% of hydrates in the system.

In 2008 Kilinc [13] investigated the dynamics of plug formation and pressure loss in a flow loop system using cyclopentane hydrates. Although Kilinc's study maintained a similar foundational structure, it was characterized by notably smaller dimensions and a different design. Such variations in experimental design offer a unique opportunity to enhance our understanding of hydrate behavior in piping systems. Given the differences in design and scale, a detailed investigation and comparison of pressure loss and plugging results between Kilinc's results and the findings in this study could provide valuable insights. Exploring these differences could help to identify how changes in system size and design affect the critical parameters of hydrate formation and plugging, thereby improving predictive models and operational strategies for managing hydrates in industrial applications.

Furthermore, this study aimed to investigate the influence of temperature, pressure, and flow rate on the formation and stability of cyclopentane hydrate plugs with different volume fractions of cyclopentane hydrates in the system. These factors play a critical role in determining the performance of hydrate-based cooling systems and must be thoroughly evaluated to ensure their practical viability. Through comprehensive experimentation and analysis, this study aims to provide valuable insight into the potential applications of cyclopentane hydrates in cooling technology, paving the way for their integration into practical cooling systems.

Chapter 2

Theory

This section presents the theoretical foundations that underpin the analysis of clathrate hydrates and fluid mechanics. Clathrate hydrates possess unique properties that make them of great interest in various scientific and industrial fields. Pressure drop, a critical aspect of fluid mechanics, plays an important role in understanding flow behavior and system performance. By investigating the dynamics of clathrate hydrates and their potential to cause pressure loss through flow obstruction, we are building a fundamental understanding that is essential for practical applications. This analysis not only helps identify how pluggings due to hydrates occur, but also serves as a critical step in the development of effective strategies to reduce these pluggings in flow systems.

2.1 Clathrate Hydrates

The experimental evidence, which can be traced back to the discovery of clathrate hydrates in the early 19th century, indicates that interactions between small non-polar molecules and water can already occur at ambient temperatures and moderate pressures, leading to the formation of ice-like crystalline structures that primarily contain water molecules[1, 14]. This section sets the stage for understanding their unique physical properties, which diverge significantly from ordinary ice, with special focus on cyclopentane hydrates. Clathrate hydrates display a variety of characteristics, including robust mechanical properties and complex behavior regarding their phase equilibrium. For a considerable period of time they have been a subject of considerable scientific fascination and pragmatic relevance, especially in the field of energy. The following sections will examine further the complexities of their structures and attributes, illuminating their possible uses and the obstacles they pose.

2.1.1 Hydrate Structures

In these nonstoichiometric hydrate structures, small guest molecules are encapsulated within hydrogen-bonded water cavities. The presence of guest molecules within the water cavities causes repulsion which expands the water cages, resulting in the formation of three distinct crystalline units shown in Figure 2.1 [14]. These types of crystal structures are known as cubic structure 1 (sI), cubic structure 2 (sII), and hexagonal structure H (sH). As presented in Table 2.1 structure I hydrates consists of two pentagonal dodecahedra cavities and six tetrakaidecahedra cavities [15]. The guest molecules have diameters ranging from 4.2 to 6 Å (Ångstrøm), such as methane, ethane, carbon dioxide, and hydrogen sulfide. In Structure II, there are 8 larger hexacahedron cavities and 16 smaller pentagonal dodecahedron cavities [15]. The smaller cavities mainly host nitrogen, hydrogen and other small molecules with diameters less than 4.2 Å. In contrast, the larger cavities accommodate single guest molecules with diameters ranging from 6 to 7 Å, such as propane or iso-butane, which also form part of Structure II. For even larger molecules, typically 7 to 9 Å, such as iso-pentane or neohexane, structure H is formed when accompanied by smaller molecules such as methane, hydrogen sulfide, or nitrogen [16].

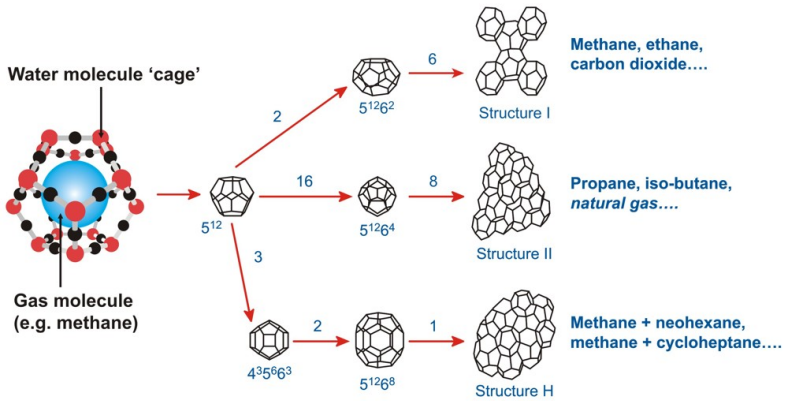

Figure 2.1: The three common hydrate structures. (Taken from HTM web site which was not copyrighted). https://hydrate.site.hw.ac.uk/what-are-gas-hydrates/. 24.03.2024

Table 2.1: Geometry of the three hydrate crystal structures. Estimates of structure H cavities from geometric models. Data in this table found in "Clathrate Hydrates of Natural Gases" by Sloan and Koh [1]. Treated and used with permission.

	Structure I		Structure II		Structure H		
	small	big	small	big	small	medium	big
Description of structure	5^{12}	$5^{12}6^2$	5^{12}	$5^{12}6^4$	5^{12}	$4^3 5^6 6^3$	$5^{12}6^8$
No. of cavities / unit cell	2	6	16	8	3	2	1
Average cavity radius, Å	3.95	4.33	3.91	4.73	3.91	4.06	5.71
H_2O molecules / unit cell	46		136		34		

Cyclopentane Hydrates

Cyclopentane is a cyclic hydrocarbon with the chemical formula C_5H_{10}. The structural composition of the molecule is a ring of five carbon atoms, each bonded to two hydrogen atoms, as depicted in Figure 2.2. The molecule consists of a five-membered carbon ring, making it a cyclic alkane. The molecular structure is relatively stable due to the equidistant arrangement of carbon atoms, which minimises stress on the ring [17]. The dimensions of the molecule is approximately 5 to 10 Å, as displayed in the top left corner of Figure 2.2. Cyclopentane is a non-polar hydrocarbon with very low solubility in water (0.0339 g/100 g at 278 K) due to the significant difference in polarity between cyclopentane molecules and water molecules [18]. The low solubility of cyclopentane in water is reflecting its hydrophobic nature and the minimal interaction between cyclopentane and water molecules.

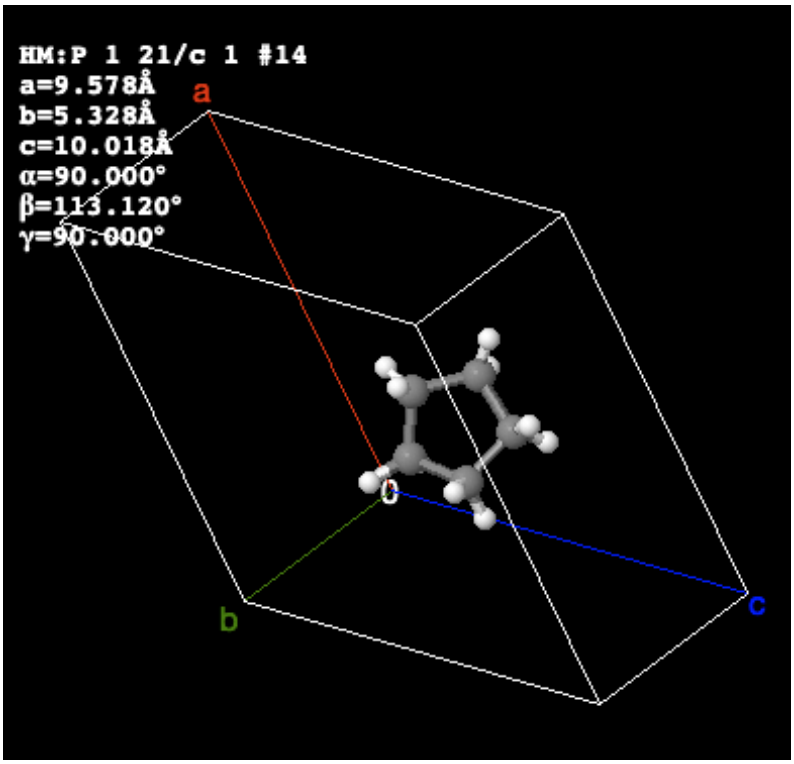

Figure 2.2: Structure of cyclopentane. Picture taken from open database www.crystallography.net/

The process of encaging cyclopentane guests in a clathrate hydrate will require the molar ratio of water and cyclopentane to be 17: 1 in sII [6]. The structure contains 136 water molecules and full occupation of the 8 big cavities for cyclopentane [19]. As shown in Table 2.1, these cavities has a structure of $5^{12}6^4$, indicating a geometric configuration composed of 12 pentagonal faces and 4 hexagonal faces [20]. Due to its size, cyclopentane is confined to the larger cavities in the sII hydrates, as it is unable to fit into the smaller cavities [21]. Figure 2.3 shows a photo of cyclopentane hydrate-water system at hydrate volume fraction of 42%, taken with microscopical camera by Kilinc [13].

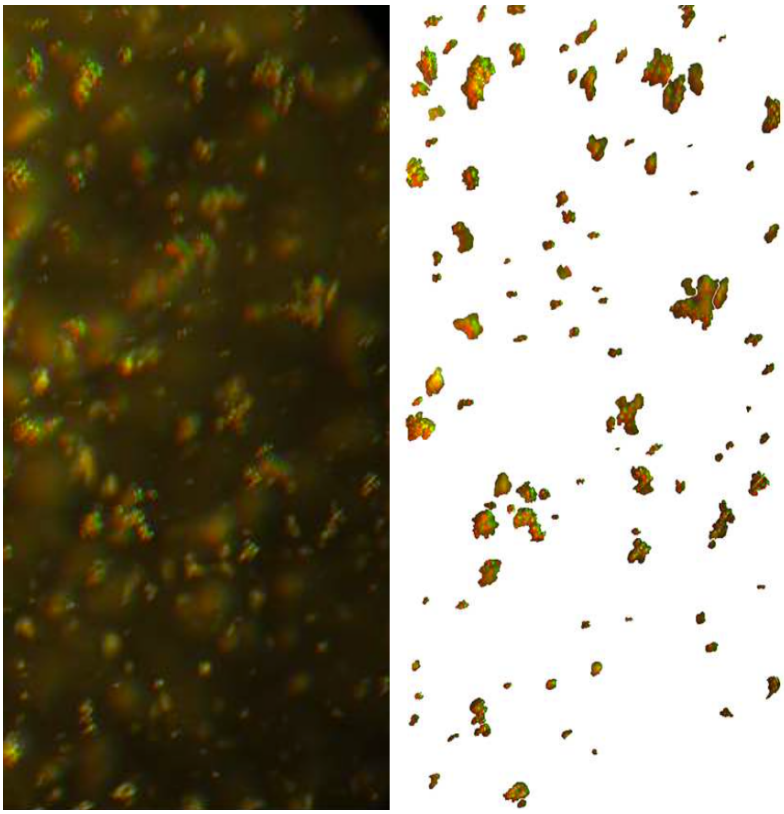

Figure 2.3: Picture of cyclopentane hydrate particles in aqueous phase, before and after removal of background noise. Picture taken from Kilinc [13] with permission.

2.1.2 Hydrate Properties

Clathrate hydrates exhibit unique properties that differentiate them from ice. For example, they possess a significant mechanical strength that may exceed that of ice by a factor of 20 times under specific conditions. This strength is attributed to the unique structure of hydrates, which includes gas molecules that provide additional binding forces within the lattice, offering greater resistance to deformation [1].

Furthermore, the thermal properties of gas hydrates contrast with those of ice as gas hydrates generally have lower thermal conductivity than ice. This property, along with their greater density compared to ice, can result in distinctive thermal behavior. For example, methane hydrates have thermal conductivity closer to that of liquid water, and their thermal expansion coefficients are significantly different from those of ice, showing an increase in volume with temperature that is influenced by the gas species within the hydrate structure [1].

Phase Equilibria and Thermodynamic Stability

The phase equilibrium of hydrates refers to the balance that occurs between the driving forces for hydrate formation and dissociation in a given liquid phase under specific temperature and pressure conditions. When hydrates form, crystalline structures of water molecules trap gas molecules, and this process depends on the temperature, pressure, and composition of the surrounding liquid.

Thermodynamic stability of clathrate hydrate is a relevant factor in their behavior since it is linked to structure under a number of different conditions. The van der Waals-Platteeuw theory was one of the first purely theoretical theories used as a fundamental tool to predict the stability conditions of clathrate hydrates using a solid solution model. This model is important in the calculation of thermodynamic properties for the stability of the hydrates at different conditions of temperature and pressure. It has been extensively used to explore and predict the behavior of different types of hydrates ever since its introduction [22].

The theory consolidates the minimum of statistical thermodynamics to understand the different contributions in the free energy of clathrate hydrates, which are those from guest-host interactions and the entropy associated with cage occupancy. The development of the theory has continued, adding anharmonic effects and lattice vibrations, to further improve the quality of predictions, particularly for hydrates involving non-spherical molecules in hydrates [23].

Phase Diagrams

The phase diagram in Figure 2.4 defines specific points known as quadruple points (Q_1 and Q_2), where four three-phase-lines intersect, so that four different phases co-exist in equilibrium [1]. Figure 2.4 demonstrates how these quadruple points divide the phase regions. The lower quadruple point, Q_1, is where the formation of hydrates ceases from vapor and liquid water, and where hydrate formation from vapor and ice begins [1]. The upper quadruple point, Q_2 marks the transition from hydrate to vapor phase with increasing temperature. This provides quantitative insight into how different components of natural gas behave under varying pressure and temperature conditions.

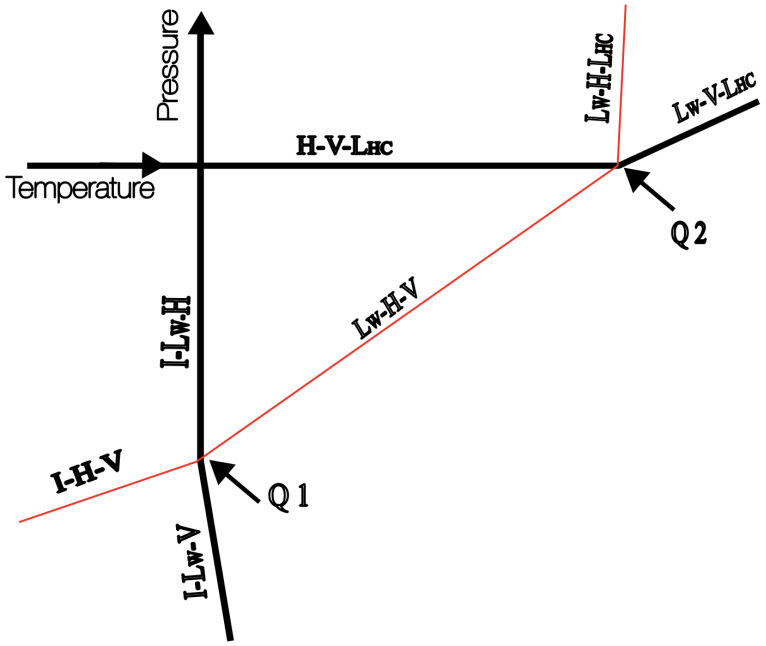

Figure 2.4: A general phase diagram for clathrate hydrates with simple hydrocarbons, such as ethane. The red curve indicates the hydrate stability zone, where hydrates are stable to the left of the curve. The pressure axis is logarithmic.

At the hydrate equilibrium curve in Figure 2.5, the rate of cyclopentane hydrate formation equals the rate of hydrate dissociation, resulting in a stable state where the amount of hydrates remains constant over time. The phase equilibrium of hydrates can vary depending on the conditions in the system. An increase in pressure might favor the formation of hydrates, while a decrease could promote their dissociation. Although lowering the temperature might drive more hydrate formation, while raising the temperature could lead to more hydrate breaking down into its component phases.

The investigation of hydrate phase equilibrium is important for comprehending and forecasting the formation of hydrates in diverse applications, such as oil and gas production, where the obstruction caused by hydrates can pose a considerable challenge. By delineating the phase equilibrium, we can devise strategies to either avert the formation of hydrates or handle hydrate-related issues efficiently, which is vital for the secure and dependable functioning of such systems.

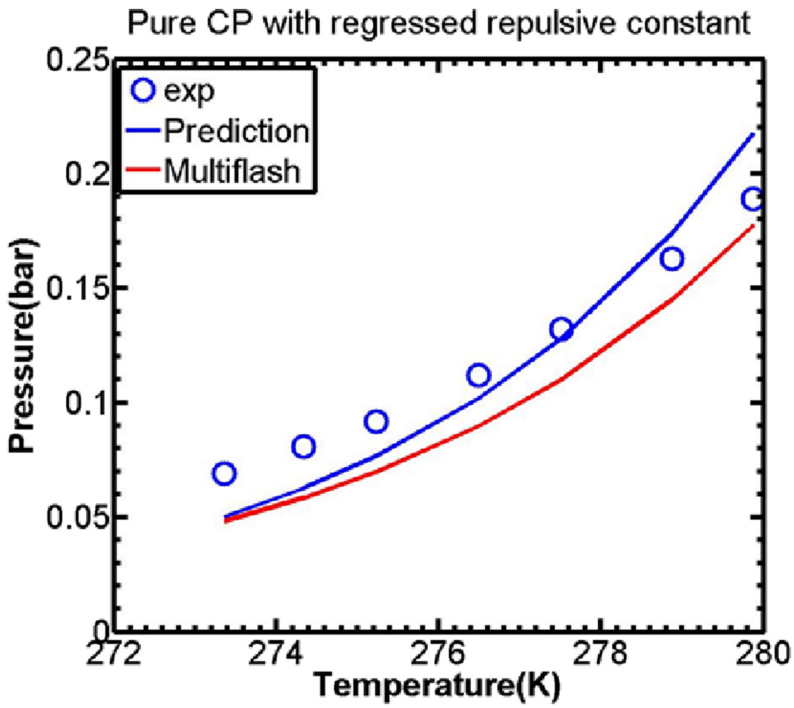

Figure 2.5: Phase equilibria prediction for pure cyclopentane hydrate compared to experimental data. Hydrate is stable in the area to the left of the curves. Used with permission from Brown et al. [24]

Although phase diagrams provide essential information about the equilibrium states of systems, they are only the first step in understanding the complex behavior of hydrate formation. In real-world applications, the dynamics of how these states are reached, through processes such as nucleation and mass transfer, are critical. Factors such as hysteresis, where the path taken to reach a phase affects the conditions for its transformation, and the kinetics of nucleation and mass transfer, which determine the rate and stability of phase changes, are vital for practical applications. These aspects are crucial to the design of systems that can effectively manage phase formation and dissociation under operational conditions.

Interfacial Tension

The interfacial tension between a hydrate and a fluid (gas or liquid) phase plays an important role in clarifying the mechanisms that regulate the growth of hydrates. It directly influences the nucleation rate of the hydrates, as it dictates the energy required to form hydrate clusters [25]. This impact of interfacial tension underscores the importance of understanding the surface properties of gas hydrates, emphasizing their relevance in hydrate formation processes.

Fluid systems with high interfacial tension will tend to separate more distinctly. Consequently, gaining insight into factors affecting the tension values is crucial for a thorough understanding of hydrate behavior.

The interfacial tension of cyclopentane hydrates and water is important to understanding their behavior in various environments, such as in oil and gas flow lines, where they can pose operational risks. Studies have determined that cyclopentane hydrate interfaces with water exhibit an interfacial tension of about 0.32 ± 0.05 mN/m, which is considerably lower than that with cyclopentane, estimated at approximately 47 ± 5 mN/m [26]. In comparison, the interfacial tension between water and ice has been measured to be 27 ± 2 mN/m, through molecular simulations [27].

The low interfacial tension between cyclopentane hydrates and water could lead to more stable hydrate formation in aqueous environments, since lower interfacial tension can mean less energy is required to form and sustain the hydrate structure. The fact also implies that cyclopentane hydrates may not dissolve easily in water, which is advantageous for applications where the preservation of the hydrate form is necessary.

The angle formed between the tangent to the liquid phase and the solid surface is known as the contact angle, which determines the wettability [28]. Wettability is a measure of how well a liquid can maintain contact with a solid surface through intermolecular interactions. If the wettability is high ($contact\ angle < 90^\circ$), the water can more easily spread and interact with gas molecules or other liquids, and hydrates will form more efficiently and have a stronger stability [29]. On the other hand, when wettability is low ($contact\ angle > 90^\circ$), water tends to bead up rather than spread out, inhibiting its interaction with gas molecules or other liquids, thereby reducing the efficiency and stability of hydrate formation.

Understanding these dynamics is crucial in areas such as enhanced oil recovery, gas hydrate management, and the design of hydrophilic and hydrophobic surfaces for industrial applications. Ultimately, using knowledge of contact angles and wettability has practical benefits, providing scientists and engineers with the tools they need to improve the efficiency and safety of processes involving multiphase interactions.

2.1.3 Cyclopentane Hydrate Based Refrigeration System

Hydrate-Based Refrigeration Systems with cyclopentane as the guest molecule (HBRS) represent an alternative approach to refrigeration technology that exploits the thermodynamic properties of clathrate hydrates. These systems work by utilising the latent heat released during the exothermic process of

hydrate formation and absorbed during the endothermic process of hydrate dissociation. HBRS typically consists of key components such as a hydrate formation tank, hydrate dissociation tank, compressor/pump, expander, and gas/liquid separator. This allows HBRS to effectively manage thermal energy transfer and storage, potentially offering higher efficiencies than traditional vapour compression refrigeration systems [3].

Studies such as Wenxiang et al. (2018), Tomohiro et al. (2006) and Xie et al. (2018) [3, 30, 31] have demonstrated the potential of HBRS to achieve excellent coefficient of performance (COP) compared with conventional refrigeration systems, making it a promising technology for future cooling needs. While the COP for traditional compression refrigeration systems usually ranges between 2 to 4, HBRS with cyclopentane has achieved COP up to 8.97 [3].

Cyclopentane in HBRS exhibits exceptional properties that enhance the performance and sustainability of these innovative cooling technologies. Cyclopentane hydrates in HBRS achieve remarkably high COP that significantly outperform conventional refrigeration systems [3], illustrating their efficiency in energy use. Cyclopentane hydrates show high efficiency for thermal energy storage and transfer [5], making them particularly suitable for applications requiring robust and reliable cooling over long periods. In addition, cyclopentane hydrates are stable at relatively low pressures compared to other hydrates [6], enabling safer and more cost-effective operating conditions. This stability not only reduces the technical challenges associated with high-pressure systems, but also enhances the overall safety and economic viability of HBRS. The studies of the subject demonstrate the potential of cyclopentane hydrates to improve refrigeration technology by providing a more efficient, sustainable and safer alternative to conventional methods.

The remarkable efficiency of HBRS makes it a greener and more economical alternative to traditional refrigeration technologies. By utilising the natural refrigerants in the clathrate hydrates, HBRS significantly reduces the environmental impact associated with synthetic refrigerants that contribute to depletion of the ozone layer and global warming [31, 32]. The potential to integrate HBRS into various sectors, particularly where cooling is required, could lead to significant reductions in energy consumption and greenhouse gas emissions. In addition, ongoing advances in HBRS technology, including improvements in system design and component efficiency, promise to increase its viability and accessibility. As the demand for sustainable cooling solutions continues to grow, HBRS stands out as a cutting-edge technology in line with global sustainability goals, offering a powerful tool in the fight against climate change while meeting the cooling needs of the future.

As mentioned, in terms of practical applications, gas hydrates have potential

as refrigerants due to their ability to maintain low temperatures, just as ice does, but over potentially longer periods due to their lower thermal conductivity. This makes them attractive for transport and storage of perishables where maintaining a consistent low temperature is crucial. Unlike ice, which melts at 0°C, certain hydrates can remain stable at higher temperatures depending on the type of gas molecule within the lattice, thus providing a refrigeration effect over a broader temperature range. This characteristic could make gas hydrates a more versatile and efficient cooling medium than ice in certain scenarios.

Building on the basic knowledge presented, it is clear that Hydrate Based Refrigeration Systems (HBRS) offers not just an alternative but a potentially revolutionary approach to refrigeration. The higher COP of HBRS, as detailed in the studies, indicates a profound efficiency that could redefine energy consumption norms in cooling technologies. This efficiency not only contributes to lower operating costs, but also meets global environmental goals by minimising the carbon footprint of refrigeration systems. In addition, the use of cyclopentane hydrates, which operate effectively at lower pressures, improves safety and reduces the complexity and cost associated with the high-pressure systems traditionally used in refrigeration.

2.2 Fluid Mechanics

Fluid mechanics is a branch of physics that deals with the study of fluids, both liquids and gases, and their behavior when subjected to various forces and conditions [33]. It encompasses a wide range of phenomena, from the motion of ocean currents and the flow of air around an airplane wing to the circulation of blood in the human body. Understanding fluid mechanics is essential for numerous engineering applications, including the design of aircraft, cars, and hydraulic systems, as well as the analysis of weather patterns and environmental processes.

Pressure drop in a fluid stream plays a vital role in fluid mechanics, especially when considering the flow within the pipes. This term is used to describe the reduction in pressure that occurs in the direction of the flow, which can be attributed to a variety of factors including friction, velocity alterations, and the characteristics of the fluid itself. Understanding the fundamental principles of pressure drop is crucial for the examination and enhancement of fluid transport systems.

2.2.1 Bernoulli Equation

Bernoulli's principle, derived from the law of conservation of energy for fluid flow, states that for an ideal fluid (incompressible and non-viscous), the sum of pressure, kinetic energy per unit volume, and potential energy per unit volume remains constant along any streamline. This equation illustrates an inverse relationship between fluid velocity and pressure; as the velocity increases, the pressure decreases, and vice versa.

Bernoulli's equation can be derived in various ways, although it is often associated with simplifications of the Navier-Stokes equations, which govern the motion of fluid substances. The Navier-Stokes equations describe the conservation of momentum and energy within a fluid, taking into account factors such as viscosity, pressure gradients, and external forces. Bernoulli's equation emerges by simplifying these comprehensive equations under specific assumptions that apply to ideal fluid flow. This derivation aligns with conditions where the fluid is incompressible, non-viscous, and flows along a streamline.

- Steady flow: This assumption implies that all conditions of the fluid at any given point remain constant over time. In other words, the flow velocity, pressure, and density do not change with time. Although this assumption is valuable for many engineering applications, it may not hold true in situations where fluid flow experiences significant fluctuations or unsteady conditions.

- Incompressible fluid: Bernoulli's principle is typically applied to fluids with constant density, meaning that changes in pressure do not significantly affect the fluid's volume. Incompressible fluids are often encountered in practical engineering scenarios, where variations in pressure are relatively small compared to the fluid density. However, it is important to note that this assumption may not be valid for highly compressible fluids or under extreme pressure conditions.

- Negligible viscous effects: Bernoulli's principle assumes that viscous forces within the fluid are negligible compared to other forces acting on the fluid. This assumption is reasonable for many fluid flow situations, particularly those involving high Reynolds numbers where inertial forces dominate over viscous forces. However, in cases where viscous effects are significant, such as flows through very small channels or highly viscous fluids, Bernoulli's equation can be adapted to include pressure loss due to viscosity and changes in piping.

The Bernoulli equation can be formulated as follows:

$$\frac{\alpha_a \overline{V}_a^2}{2} + \frac{p_a}{\rho} + gz_a + \eta W_p = \frac{\alpha_b \overline{V}_b^2}{2} + \frac{p_b}{\rho} + gz_b \tag{2.1}$$

In presented equation, α represents the kinetic energy correction factor, $\overline{V}$ is the average velocity in meters per second, and ρ stands for the density in kilograms per cubic meter. The variable p indicates the pressure in pascals, η is the pump's efficiency as a dimensionless factor, and g denotes the acceleration due to gravity in meters per second squared. The z_j values signify the height at various points along the flow path in meters, and W_p quantifies the work done by the pump in joules per kilogram.

The kinetic energy correction factor, denoted by α is the ratio between the actual kinetic energy flowing through a normal cross-section and a uniform velocity profile flowing through the same cross-section. This factor varies depending on the flow regime; for fully developed laminar pipe flow, it is around 2, whereas for turbulent pipe flow it ranges from 1.04 to 1.11 [34]. When included in the complete equation for the incompressible steady flow energy, α allows the generalization of the equation to accommodate real flow conditions, encompassing elements such as pumps, turbines, and frictional losses.

2.2.2 Reynolds Number

Reynolds number is a dimensionless quantity that plays a crucial role in fluid dynamics, particularly in determining the type of flow regime a fluid experiences within a conduit or around an object. Named after Osborne Reynolds, who introduced the concept in the late 19th century, it represents the ratio of inertial forces to viscous forces in a flowing fluid. Mathematically, it is expressed as follows:

$$Re = \frac{\rho v L}{\mu} \tag{2.2}$$

Where ρ is the fluid density, v is the fluid velocity, L is the characteristic length scale of the flow (such as the pipe diameter), and μ is dynamic viscosity of the fluid [34].

The Reynolds number serves as a fundamental parameter in fluid mechanics, providing insights into the behavior of flowing fluids. It helps classify flow

regimes into laminar, transitional, or turbulent based on the relative importance of inertial and viscous forces. In laminar flow, characterized by smooth and orderly fluid motion, the Reynolds number is typically low ($Re < 2300$). Transitional flow occurs as the Reynolds number increases ($2300 < Re < 4000$), leading to a mix of laminar and turbulent characteristics. Turbulent flow, where the motion of the fluid is chaotic and irregular, occurs at high Reynolds numbers ($Re > 4000$).

The degree of turbulence affects the hydrate slurry. In more laminar flows ($Re < 300$), there is a more homogeneous distribution of hydrate particles, which is a state of more similar sized particles evenly distributed throughout the system. When there is more turbulence in the flow ($Re > 300$), the hydrate particle distribution is more heterogeneous, causing the hydrate particles to form clusters or plugs [35]. Building on the dynamics of hydrate slurries in different flow regimes, it is important to explore how these behaviors affect practical applications, especially in industries where precise control of fluid dynamics is critical, such as oil and gas pipelines and refrigeration systems.

2.2.3 Rheology and Molecular Interactions

In the study of materials and fluids, it is essential to understand the fundamental forces that govern the behavior of molecules. Among these, adhesion and cohesion are key intermolecular forces that determine how substances interact with each other and their environment. Adhesion refers to the attractive force between different substances, such as water molecules clinging to glass, while cohesion describes the attraction between like molecules, such as water to itself. These forces are critical in a wide range of applications, from the design of adhesive products to the flow of liquids in industrial processes.

Van der Waals forces is important in understanding adhesive and cohesive forces. The van der Waals forces are a type of weak intermolecular force that mainly include three types, which are dispersion forces. dipole-dipole interactions and induced dipole interactions. In adhesion, the van der Waals forces act in the surface interactions, and when the surface is smooth, the van der Waals forces act stronger as the contact area is maximised. Van der Waals forces play an important role in cohesion that promotes particle aggregation [36].

Adhesion

In the case of hydrates, adhesion describes the interaction between the hydrate particles and other surfaces, such as the walls of the pipeline or other solid materials. The adhesion force between clathrate hydrates and pipeline surfaces will be significantly influenced by the material of the surface and the surface energy. Hydrates adhere more strongly to surfaces with high surface energy, such as metal surfaces, than to surfaces with low surface energy, such as coated surfaces [37].

The presence of water significantly affect the adhesive force, sometimes in a seemingly contra intuitive way. Aspenes found that when water is present where oil or gas is the primary phase, it can form capillary bridges between the hydrate particles and the surface, increasing adhesion [38]. For example, the adhesive forces between cyclopentane hydrates and solid surfaces increased by more than 10 times in water-wet conditions compared to dry conditions [38].

Nicholas et al. [7] conducted measurements of adhesive forces between various materials, including cyclopentane hydrates, ice, and carbon steel (1μm and 240 grit). Their findings revealed that the adhesive force between ice and carbon steel, under subcooling ranging from 1 to 7 °C, varied from approximately 1.37 to 2.77 μN, showing an increase with rising temperature. The contact force between cyclopentane hydrates and carbon steel was measured to be about half of the ice values at similar subcoolings, hypothesized to be dominated by capillary forces. Generally, these capillary forces originate from the presence of a quasi-liquid layer on the surface of the solid phase. [39, 40]. One expect that a temperature increase will results in a thicker quasi-liquid layer, thus raising the adhesive force between hydrate/ice and carbon steel, which is consistent with the results conducted by Nicholas et al. [7].

Adhesive forces between clathrate hydrates and pipeline surfaces play a critical role in hydrate management. Effective mitigation strategies, including surface coatings and moisture control, can significantly reduce these forces and prevent hydrate-related blockages. Understanding these mechanisms will allow better design and operation of pipelines in hydrate-prone environments.

Cohesion

In the context of clathrate hydrates, cohesion describes the forces that hold hydrate particles together. These forces play a crucial role in the aggregation of hydrate particles, which can lead to the formation of plugs in pipelines. There are several factors that are influencing the cohesive forces between hydrate particles such as capillary bridges and sintering. Also, higher surface free energy of particles increases the cohesive forces between them [41]. Nicholas

et al. [7] also measured the contact forces between cyclopentane hydrates themselves, which was approximately 2.0 - 6.1 μN at subcooling between 2 and 6 °C.

In settings where hydrate particles are exposed to a liquid phase, capillary bridges can form between the particles. These bridges, composed of either liquid water or a water-hydrocarbon mix, create attractive forces that pull the particles together. Such capillary forces markedly enhance the cohesion among hydrate particles, facilitating the sintering between asperities mechanism, especially in the presence of guest molecule liquid phase such as cyclopentane [42]. Sintering occurs when particles partially fuse at points of contact, forming solid bridges. This process becomes increasingly significant as hydrate particles remain in proximity over extended periods of time, allowing the growth of solid bridges that increase cohesion [36]. It has been found [42] that this increase in annealing time, makes the surface of hydrate particles rougher, resulting in a decrease in cohesive forces.

Chapter 3

Methodology and Experimental Apparatus

The methodology employed in this study encompasses a systematic approach aimed at investigating the formation and behavior of cyclopentane hydrates within the experimental setup. This chapter provides a comprehensive overview of the methods and procedures utilized, separated into several key sections.

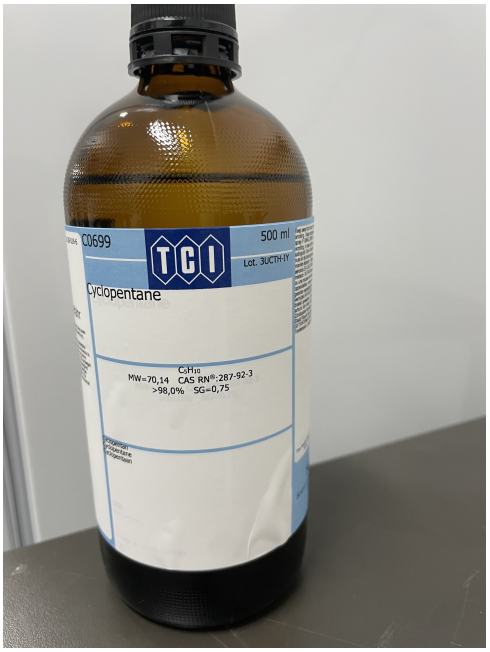

Figure 3.1: Cyclopentane delivered by TCI Europe

The cyclopentane utilized in the experiments is sourced from TCI (Tokyo Chemical Industry) Europe, see Figure 3.1, ensuring a purity level exceeding 98%. At the core of the experimental setup lies the intricate design and operation of the flow loop shown in Figure 3.2. This section explains the configurations and functionalities of the flow loop, which is the backbone for conduction of experiments. By detailed description, it offers insight into of how important the part of the flow loop is in order to provide controlled flow conditions and data collection.

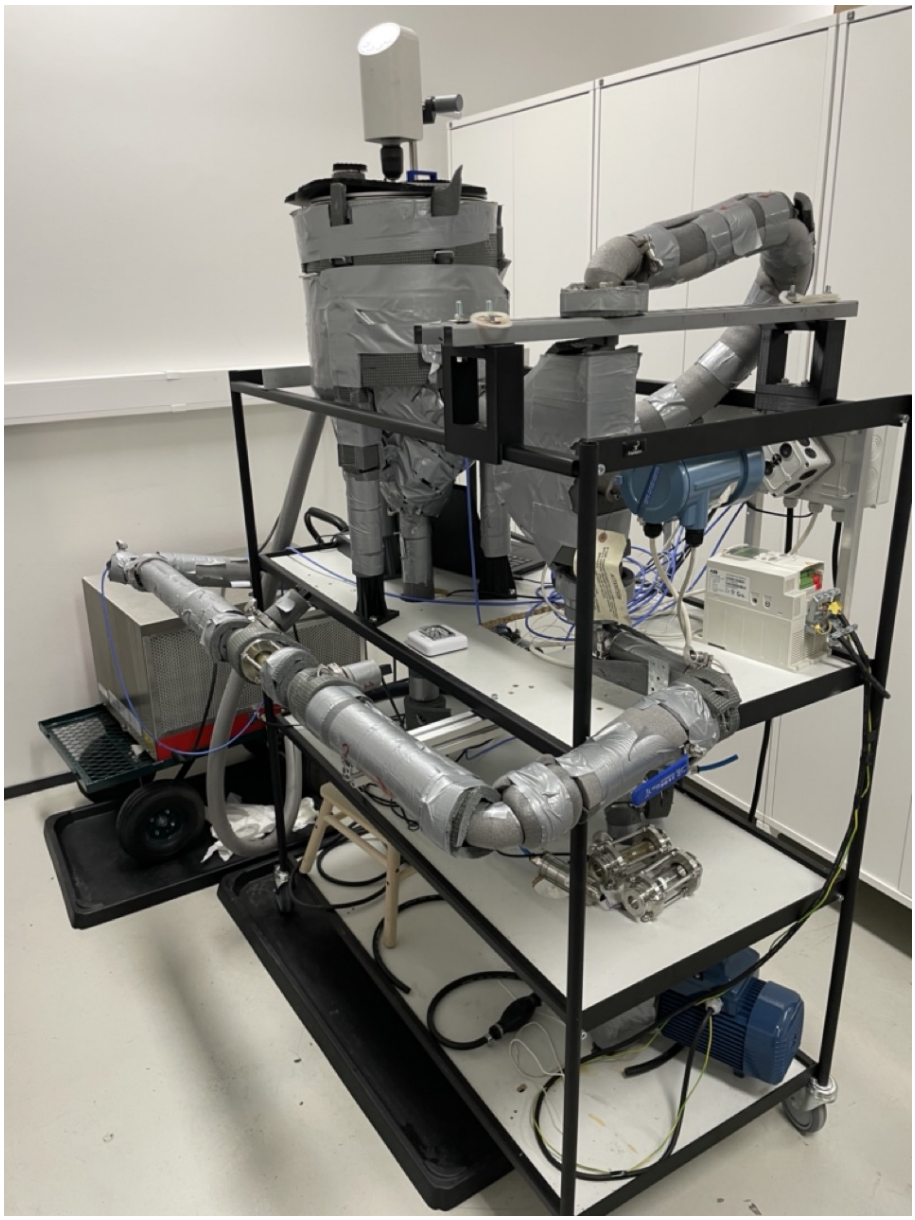

Figure 3.2: Overview of the flow loop.

Methodical preparation is crucial for ensuring the reliability of experimental results. This section outlines the specific preparatory steps undertaken to ready the experimental setup. These steps include constructing the experimental apparatus, addressing challenges faced during the setup process, and performing detailed calculations to determine system parameters. Each of these aspects plays a vital role in preparing for and conducting the experiments effectively.

The experiments conducted to investigate different aspects of gas hydrate formation and behavior are central to the study. This section is divided into sub-sections, each focusing on a specific experiment conducted within the framework of the study. From exploring pressure drop phenomena to analyzing sample behavior over time and inducing blockages to assess hydrate formation dynamics, these experiments collectively contribute to a comprehensive understanding of gas hydrate interactions within the system.

By delineating these key components, this chapter sets the stage for a detailed exploration of the experimental methodology employed in the study, laying the groundwork for analyses and findings.

3.1 Flow Loop

The experimental arrangement is illustrated schematically in Figure 3.3. It involves a closed-loop flow system. The fluid in the system is pumped through a test section, which is depicted in Figure 3.4, that comprises a straight horizontal pipe, measuring 1.73 meters in length , with an inner diameter of 22 millimeters and a wall thickness of 1.5 millimeters. The walls of the tubing are constructed of durable 304 stainless steel. To place a temperature sensor at the entrance to the test section, a blind-T flow restriction is placed. Furthermore, an orifice, with dimensions of 9.5 millimeters in diameter and 10 millimeters in length, is incorporated to increase the likelihood of plug formation. Additionally, the orifice is equipped with two facets measuring 1 millimeter by 45 degrees to optimize its performance.

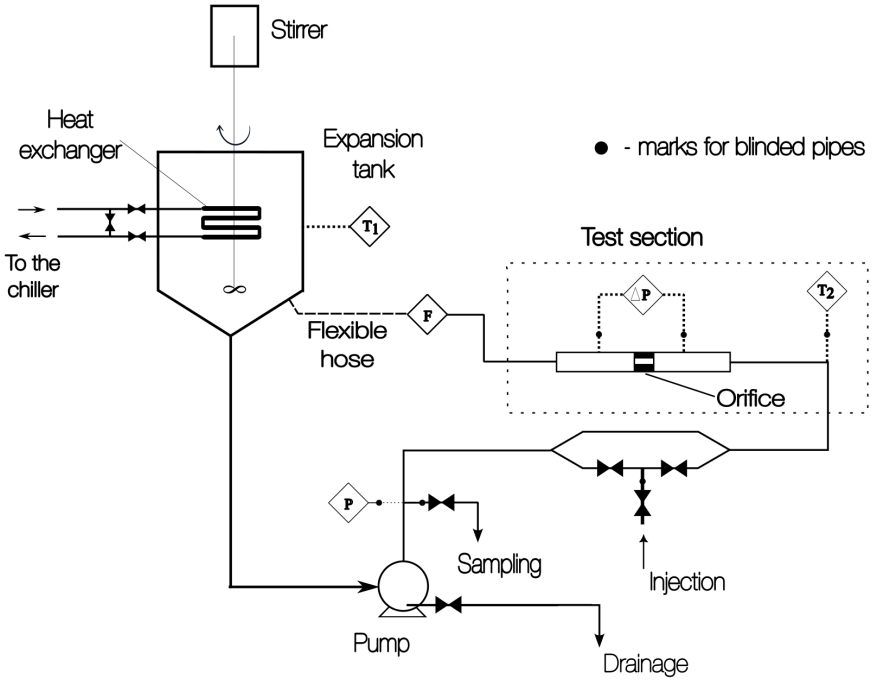

Figure 3.3: The hydraulic scheme of the flow loop. P, T, F denote pressure, temperature, and flow rate measurements. Blinded pipes are used for housing sensors or facilitating specific functionalities such as bypasses (outlet) and injection points (inlet).

Installed at a distance of 850 millimeters from the input of the test section, the orifice corresponds to 38.6 hydraulic diameters and is encased within a 110-millimeter transparent glass pipe composed of borosilicate glass 3.3, allowing visual monitoring. Total length of steel piping employed throughout the loop is 6.7 meters. Furthermore, the loop includes various bends and bifurcations, along with an injection port, to ensure precise control and manipulation of the experimental conditions.

To pump the slurry, a centrifugal pump (Pedrollo HF 70 A, 2.2 kW) is installed in conjunction with a frequency converter (ABB ACS355), which facilitates the adjustment of flow within the system. The pump casing was made from cast iron, whereas the impeller, featuring a closed-type design, is made from brass. With an axial clearance of 4 mm, the impeller, equipped with seven blades, boasted a thickness of 10 mm and a diameter of 200 mm.

The flow loop measurement apparatus included a digital manometer located at the pump outlet, a differential manometer stationed in the test section, a Coriolis mass flow meter installed downstream of the test section, and multiple temperature control sensors. Using additional computer tomography,

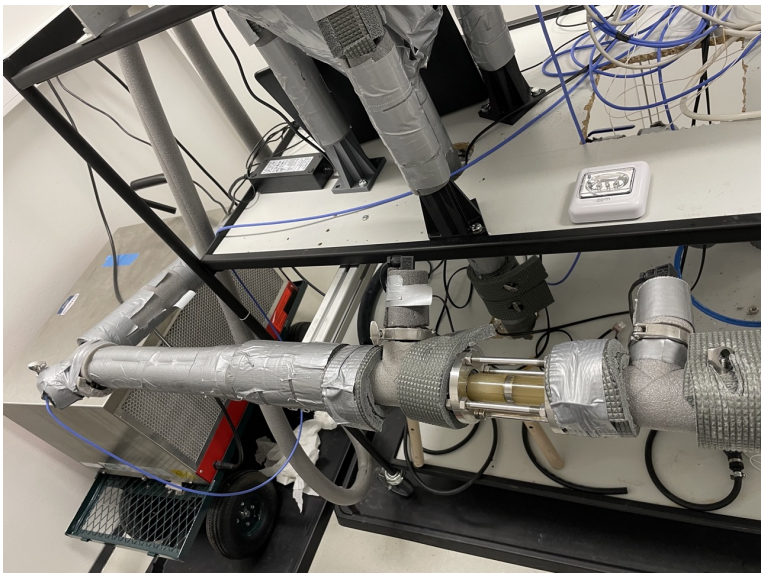

Figure 3.4: The test section, where measurements of temperature and pressure are taken. The sensor attached to the blue cable in the far left of the picture takes measurements of temperature at the corner before the orifice, and pressure is measured right before and after the orifice.

the internal channel geometries of the flow meter were elucidated. Detailed specifications of the measurement system are outlined in Table 3.1. Data from these sensors were captured and processed using the National Instrument 6001 DAQ USB data card, managed through a LabView-based control program with a sampling frequency of 1 kHz. The script can be seen in Appendix A.

Furthermore, the flow loop incorporated an expansion tank, crafted from durable 304 stainless steel and openly exposed to the atmosphere. This tank served multiple functions, including filling, cooling, and dispersion of the slurry. Structurally, the tank consisted of a cylindrical top section (with a diameter of 310 mm and a height of 310 mm) and a conical bottom section (with a diameter of 35 mm at the bottom and a height of 230 mm), with a total volume capacity of 29.9 liters. Inside the tank, a coil heat exchanger, constructed from SS 304 metal pipe (with dimensions of 10 $\times$ 1 mm), facilitated efficient cooling. This heat exchanger featured fourteen coils of a rectangular rounded shape, measuring 120 $\times$ 50 mm each, with a radius of 25 mm. To regulate the temperature within the tank, the cooling system incorporated a bypass line, which allowed adjustment of the coolant flow rate. This meticulous control ensured the accuracy of the temperature within $\pm$ 0.2 $^\circ$ C relative to the required temperature. The coolant utilized was a 35 vol% propylene glycol - water mixture, which was efficiently circulated by the Y 2051.0263 pump,

Table 3.1: The measurement system of the flow loop. Data found in Struchalin et al. [9] Used with permission.

Parameter	Sensor	Meas. range	Instr. error
Temperature	PT100 + LKM 103 Transducer	$-40 \sim 85°C$	$\pm 0.1°C$
Pressure	Gems 3500 Pressure Transmitter	$0 \sim 4bar$	0.25%
Differential pressure	Omega PXM219-006AI	$0 \sim 6bar$	0.25%
Flow rate	Micro Motion Coriolis Flow Meter (R050S Sensor,1700 Transmitter)	$0 \sim 3600kg/h$	0.5%

delivering a flow rate of 0.44 m^3/h.

To homogenize the slurry during the testing, an overhead stirrer (Joanlab OSC-20L) equipped with a 75 mm three-blade impeller continuously operated at 1400 rpm. Furthermore, thermal insulation was provided by two layers of polyethylene foam, effectively mitigating heat exchange with the surroundings. The average thermal resistance of the walls was 5.3 $(m^2 \cdot K)/W$. The experimental setup was housed in a controlled environment, managed by an automatic energy management system, maintaining a stable room temperature ranging between 21.2∼25.4°C.

3.2 Preparations

In the preparations phase, significant effort was dedicated to completing the unfinished flow loop, depicted in Figure 3.5 close to its original state. This involved careful assembly and integration of various components, such as valves, pipes, and fittings, to establish a closed-loop system capable of circulating the desired fluids under controlled conditions. Special attention was given to securing the proper alignment and sealing of connections to prevent leaks and maintain system integrity. Insulation was carefully applied throughout the flow loop to minimize heat energy flow into the system, ensuring optimal operating conditions for the experiments. Once the flow loop was completely built, it was flushed with water and red spirit.

Figure 3.5: The flow loop under construction. Visibly, there are several open ends in the piping.

Furthermore, extensive calibration and testing procedures had to be conducted to verify the performance and accuracy of the measurement systems integrated into the test section. This included calibration of pressure sensors, flow meters, and temperature probes to ensure reliable data acquisition throughout the experiments. Familiarization with the operation of all system components, including the pump, chiller, stirrer, and connections from the sensor to the data acquisition unit for signal reception, was essential for operating the flow loop properly and safely. Furthermore, adjustments were made to the LabVIEW

code, originally developed by Struchalin et al. [9], to align with the setup of the flow loop. Additionally, extensive reading on clathrate hydrates and cyclopentane was undertaken to enhance understanding of the subject.

Challenges

There were some hurdles that had to be addressed to ensure the smooth execution of the experiments. An incident occurred after the completion of the flow loop assembly when it was time to fill it with water for leak testing. Unexpectedly, leakage was observed originating from the tank. Initially, the source of the leak was unclear, but was eventually traced back to a faulty connection between the tank and the inlet pipes. This connection, designed inadequately to accommodate the curvature of the tank, required the fabrication of a new part to prevent further leakage. Delays ensued as some components had to be imported from Belgium.

Another significant challenge arose with the discovery of rust within the system. The cause of the rust was initially ambiguous, but it was later determined that the stirrer had been scraping against the tank lid where it passes through. Metal dust was observed around this area, indicating it as a primary source of rust formation. Subsequently, the system was drained and flushed multiple times to mitigate the issue. Measures were implemented to prevent further frictions between the stirrer and the tank lid, such as regularly tightening the nut between the lid and the stirrer stand and limiting the stirrer speed to below 1500 rpm as it exhibited too much vibrations above that rotational speed.

Calculations

To determine the appropriate volume of cyclopentane required to achieve a desired ratio of liquid water to hydrates in the system, it is essential to calculate the volume occupied by the hydrates. The process of hydrate formation involves the extraction of water from the system, which must be included in the calculations.

In the calculations as follows, n_j represents the number of moles for component j, the symbol V_j denotes the volume, and Mm_j stands for the molar mass. C_{hyd} indicates the volume fraction of hydrates in the system and ρ_j symbols the density of component j. The notation employed in the documentation uses various subscripts to denote specific components and characteristics within the system. Here hyd refers to the hydrate component, cp designates cyclopentane, and w indicates water. The subscript $w,\ hyd$ is particularly used

to denote water that is incorporated within the hydrates.

There are some preconditions and assumptions for the system that need to be considered in the calculations:

- The hydrate structure sII will only form with 8 large cavities for cyclopentane per hydrate unit. As shown in Table 2.1 there will be 136 H_2O molecules per each hydrate, corresponding to stochiometric ratio of 1:17 of cyclopentane and water in the hydrates [6].

$$\frac{n_{\text{cp}}}{n_{\text{w, hyd}}} = \frac{1}{17} \tag{3.1}$$

- There will be a 100% conversion of cyclopentane to hydrates
- The density of cyclopentane (compressible fluid) under relevant conditions is 751 kg/m^3 [43]
- The density of the hydrate is 954 kg/m^3 [44]

To calculate the necessary amount of cyclopentane to introduce into the system, to get a desired ratio between liquid water and hydrates within the system, there needs to be some defining equations to work with. Then, by combining various equations, the equation for the required amount of cyclopentane is found. The path to get the following equation can be found in Appendix B. The required volume of cyclopentane is found through this equation.

$$V_{\text{cp}} = \frac{C_{\text{hyd}} \cdot V_{\text{tot}} \cdot Mm_{\text{cp}} \cdot \rho_{\text{hyd}}}{(Mm_{\text{cp}} + 17 \cdot Mm_{\text{w}}) \cdot \rho_{\text{cp}}} \tag{3.2}$$

Equation 3.2 depends on V_{tot} to calculate V_{cp}. This makes it not a fully independent equation, because V_{tot} is not a fixed value and varies depending on the value of V_{cp}. However, there is a simple solution to this problem. By iterating V_{tot} based on the latest result of V_{cp} three times, the difference between the iterations becomes less than 0.001 L.

To do the iterations, an assumptions that V_{tot} is the same volume as the amount of water which is added in the flow loop. By using Equation 3.2 we obtain a volume of cyclopentane. With that volume, we need to find out how much the volume of the system would increase by after the hydrate formation from the cyclopentane. To calculate this, first find out the number of moles in the given volume of cyclopentane. Then calculate the volume of the formed hydrates with the following equation:

$$V_{\text{hyd}} = \frac{n_{\text{hyd}} \cdot Mm_{\text{hyd}}}{\rho_{\text{hyd}}} \tag{3.3}$$

Then, the volume of the liquid water already in the system that now forms hydrate cages needs to be subtracted from the total volume of the system while the volume of the hydrates is added. The increase in volume of the system is calculated from the following equation.

$$V_{\text{tot, i+1}} - V_{\text{tot, i}} = V_{\text{hyd, i}} - \frac{136 \cdot n_{\text{hyd, i}} \cdot Mm_{\text{w}}}{\rho_{\text{w}}} \tag{3.4}$$

After calculating the increase of the total volume of the system, add the increase to V_{tot} in Equation 3.2. Then, a new value for V_{cp}, will be further iterated until the difference between the iterations satisfies the accuracy criteria. An example of calculating the necessary amount of cyclopentane to be added can be found in Appendix B

3.3 Experiments

The experiments in the flow loop followed a standardized protocol: Initially, the chiller is calibrated to 1°C. This temperature setting was chosen based on the estimated phase diagram of cyclopentane hydrates shown in Figure 2.5, where Brown et al. [24] have conducted an assessment of the phase equilibrium of cyclopentane hydrates, employing both theoretical and empirical techniques. It can be observed that hydrate stability is maintained above the equilibrium line, whereas if the conditions descend below the line, the hydrates will dissociate. This is important for the ability to sustain prolonged subcooling within the rig, thereby maximizing particle cohesion.

A specific amount of Cyclopentane is added, in order to get a desired volume fraction of hydrates in the system. This amount is decided by using the equations 3.2 - 3.4. The stirrer is activated and the pump starts the operation at a flow rate of around 1000 kg/h. To ensure a near-complete conversion of cyclopentane to hydrates, the flow is allowed to run for one hour under these conditions.

Pressure Drop

The pressure drop in the flow in the test section (see Figure 3.4), was examined at various pump frequencies (5 Hz – 11 Hz). This investigation aimed to assess the effect of different pump frequencies on the flow characteristics and pressure drop within the system. By analyzing the pressure drop under varying operating conditions, insights into the behavior of the cyclopentane-in-water hydrate slurry could be gained, providing valuable information for optimizing flow conditions and system performance. Throughout each experiment with different volume fractions, data acquisition was facilitated through the LabVIEW script, allowing monitoring and analysis of system responses to varying parameters.

The first flow experiment contained 640 ml of pure cyclopentane, which result in a 9.45 vol% of hydrates in the system, by using the equations in Chapter 3.2. At this volume fraction in the system, some hydrate particles started to appear in the flow, but very few. The volume fraction of hydrates within the system was further increased to 14 vol% to assess its impact on flow behavior and pressure drop. One could clearly see hydrate particles in the system. The temperature of the system was adjusted to about 0°C to ensure hydrate stability in further experiments.

Further, increasing the volume fraction to 22.1%. At this stage, a decision was made to explore higher pump frequencies to examine the evolving pressure drop curves at increased flow rates. This adjustment prompted a shift in pump frequencies from 5 Hz to 15 Hz, with the aim of exploring the effects of higher flow velocities on pressure drop dynamics. The volume fraction was further raised to 25.8%, 35%, 40%, 45% and 50%.

Overall, the progressive increase in the volume fraction of hydrates, enabled a comprehensive exploration of flow characteristics and pressure drop phenomena, offering valuable insights into the behavior of cyclopentane-in-water hydrate slurries under varying operating conditions. These findings lay the groundwork for optimizing flow conditions and enhancing system performance in practical applications.

Emulsion Samples

In an experimental setup, two samples of the cyclopentane and water-emulsion were extracted from the system containing a 3.3 vol% of cyclopentane: one from the main tank and the other from a bypass. The amount of cyclopentane would in theory (based on the calculations in Chapter 3.2) eventually result in 14 vol% of hydrates in the samples. The sample from the main tank may be a more homogeneous composition compared to the one from the bypass.

This disparity in homogeneity is due to the different flow dynamics of the fluids in the tank and bypass. The difference in viscosity between the fluids may influence which fluid is more prone to exit the bypass more readily. Additionally, the buoyancy effects of cyclopentane, being lighter than water, might cause it to ascend more readily, resulting in a denser volume fraction of cyclopentane from the tank compared to the bypass.

Subsequently, both samples were placed in a refrigerator maintained at temperatures between 2 to 4 degrees Celsius for several days, depicted in Figure 3.6. This temperature range was chosen to mimic the conditions conducive to hydrate formation. This experiment aimed to evaluate the propensity of hydrate formation in the cyclopentane-in-water emulsion under controlled cooling conditions, providing insights into the stability and behavior of the system over time. Over the observation period, there were not any occurrence of hydrate formation within the samples.

Figure 3.6: Samples. Left samples is from the bypass and the right sample is from the tank

Stable Flow Over Longer Time

In an experimental scenario following the formation of hydrates, the flow was allowed to continue uninterrupted for a duration of 7 to 8 hours. This experiment was designed to assess whether the hydrate slurry could be stored for an extended period without destabilizing the flow. During this period, key aspects were evaluated, including the flow rate, pressure, and temperature profiles throughout the system. Monitoring these parameters helped to gauge

the efficiency of the flow process and to determine whether the presence of hydrates induced any significant changes or instability.

The overall purpose of the experimental setup was to gain a comprehensive understanding of the long-term behavior and performance of hydrates in a flow system, specifically looking at their potential for prolonged storage in energy applications. The observations from this experiment indicated that the flow remained stable and was not destabilized by the hydrate presence. This contributed valuable insights into the long-term stability and operational dynamics of hydrate-based systems.

Blockage

In an experimental setup aimed at creating a blockage in the test section, the objective was to induce hydrate formation and subsequent plugging. The process began by operating the flow loop at a temperature of 1-2 °C and a flow rate just below 1000 kg/h for a duration of one hour. This initial phase was aimed at converting nearly 100% of the cyclopentane into hydrates within the system.

Subsequently, the flow rate was reduced to around 100 kg/h to facilitate favorable conditions for blockage formation. This reduction in flow rate corresponds to lower Reynolds numbers, indicating a transition towards laminar flow regimes. At lower Reynolds numbers, flow conditions promote the agglomeration of hydrate particles, increasing the likelihood of plug formation within the flow conduit. The Reynolds number is calculated by Equation 2.2, which for 100 kg/h results in a Reynolds number of about 1 600. Throughout the experiment, observations were made to monitor the formation of blockages and the behavior of the hydrates within the flow loop.

Initially, the volume fraction of hydrates in the system was set at 14%. This was based on earlier experiments performed by Balakin and Stuchalin [10] where the ice slurry made a blockage with 100% certainty at this volume fraction. No blockages were observed, indicating that the hydrate formation process did not lead to immediate plugging. However, over time, additional cyclopentane bubbles appeared within the system. This observation suggested that a portion of the hydrates had dissociated back into water and cyclopentane, indicating a dynamic equilibrium between hydrate formation and dissociation. This dynamic process demonstrated the complex interaction between hydrate formation, dissociation, and flow dynamics within the system. Overall, the experiment provided valuable insights into the transient behavior of hydrates and their impact on flow blockage formation in pipelines.

Following the initial phase of the experiment, additional cyclopentane was

introduced into the system, to reach 16 vol% of hydrates. The temperature was adjusted from 1 to 0 °C to maintain suitable conditions for the stability of the hydrate. Observations during this phase revealed that, although there were no visible cyclopentane droplets within the system, there was still no formation of blockages in the test section. Despite the increase in the percentage of hydrate volume in the system, the flow dynamics did not result in plugging.

To further investigate the blockage formation potential, additional cyclopentane was introduced into the system, bringing the hydrate volume fraction to 18.2 vol%. At this volume fraction, no obvious changes were observed, with only minor accumulations of hydrate particles noted at the top of the test section.

Continuing the experimentation, the volume fraction was raised to 25.8%. Throughout this phase, careful observation showed no indications of blockages or significant changes in system behavior. Instead, the observations primarily highlighted the formation of dispersed hydrate accumulations within the flow, particularly evident at the test section's upper regions. Similar observations were made in the volume fraction of 35%.

In the experiment phase with a 40% volume fraction of hydrates, the flow was set at around 90 kg/h. Over a span of 40 minutes, the flow rate gradually declined towards zero, eventually reaching a complete halt. This significant reduction in flow velocity indicated a substantial hindrance to fluid movement within the system.

In an attempt to induce blockage formation at this volume fraction, further investigations were conducted by varying the flow rate. Starting with a higher flow rate, the flow rate was gradually decreased until the point where the blockage occurred. Interestingly, at a flow rate initially around 135 kg/h, the formation of a blockage became evident as the pipes became increasingly obstructed, and the flow rate declined to 0 kg/h. This observation underscores the critical role of hydrate volume fraction in influencing flow behavior and blockage formation. At higher volume fractions, the propensity for blockage becomes more pronounced, as evidenced by the gradual reduction in flow velocity and eventual obstruction of the flow path.

In subsequent phases of the experiment, the hydrate volume fraction was increased to 45% and 50% to further explore the conditions leading to plugging. The purpose of these increments was to assess whether higher concentrations would exacerbate the tendency to plug. However, observations at these higher volume fractions showed little deviation from the behavior observed at 40%. Despite the increased presence of hydrates, the flow characteristics and plugging results remained consistent with previous observations. This suggests that the system may have reached a saturation point beyond which additional

hydrates do not significantly affect the likelihood of blockage, or that the dynamics of hydrate interaction and accumulation at these concentrations do not further contribute to flow obstruction.

In conclusion, the experimental investigation of blockage formation by varying hydrate volume fractions has provided valuable insights into the dynamics of hydrate behavior in pipeline systems. The critical volume fraction for blockage appears to be around 40%, where a noticeable reduction in flow rate and eventual cessation of movement indicates significant obstruction. Beyond this point, further increases in hydrate concentration did not lead to more severe blockages, suggesting a limit to the effect of hydrate accumulation on flow obstruction under the conditions tested. These results highlight the importance of closely monitoring and controlling hydrate concentrations in pipeline systems to prevent operational disruptions and ensure efficient flow management. This research contributes to our understanding of hydrate-related flow problems and assists in the development of more effective strategies for managing such challenges in hydrate-prone systems.

Chapter 4

Results and Discussion

This chapter delves into a comprehensive analysis of the outcomes obtained from the last chapter. It examines the results in terms of pressure drop, blockage formation and potential applications of hydrates. Through a systematic review of these results, accompanied by critical reflection, this chapter aims to unravel the lessons learned from the experiments conducted. It navigates through the observed trends, discrepancies and implications arising from the data, in order to get a deeper understanding of the behavior of cyclopentane hydrates.

4.1 Pressure Drop

In the analysis of pressure drop within the flow loop, the experimental results revealed distinct trends that provide valuable insights into behavior of cyclopentane-in-water hydrate slurries under varying flow rates and hydrate volume fractions in the system.

As shown in Figure 4.1 (a), the pressure drop curves exhibit consistent patterns across different volume fractions, indicating a relatively stable behavior of the hydrate slurry under varying conditions. However, closer examination reveals subtle differences that correspond to changes in volume fraction of hydrates. As the volume fraction of hydrates increases, there is a noticeable decrease in the flow rate. This observation suggests that higher volume fractions of hydrates contribute to increased resistance to flow within the system, resulting in slower flow rates.

In Figure 4.1 (b), the increase in pressure drop is shown compared to the pressure drop where there was no cyclopentane in the system, only pure water. The increase is found by Equation 4.1, here $\dot{m}$ is the mass flow rate, ΔP_i is the pressure drop with pure water, and with index $i+1$ indicating cyclopentane in the system. It is important to note that the pressure drop is normalized by

the mass flow rate rather than simply comparing pressure drops directly. This normalization is crucial because the pressure drops are measured at varying flow rates. Directly comparing pressure drops without considering the flow rate variations would not accurately reflect the relative increase.

$$Increase = 1 - \frac{\frac{\Delta P_{i+1}}{\dot{m}_{i+1}}}{\frac{\Delta P_i}{\dot{m}_i}} \tag{4.1}$$

Furthermore, the comparison of pressure drop curves at different pump frequencies elucidates the dynamic nature of flow behavior. At lower pump frequencies, corresponding to lower flow velocities, the pressure drop remains relatively constant across different volume fractions. However, as pump frequencies increase, indicative of higher flow rates, the pressure drop curves exhibit more pronounced variations, particularly at higher hydrate volume fractions.

A significant finding emerges when examining the pressure drop behavior at higher hydrate volume fractions. At volume fractions approaching 40%, there is a dramatic decrease in flow velocity, leading to a drastically increased pressure drop. This phenomenon suggests a critical threshold at which the presence of hydrates significantly impedes flow, resulting in a significant reduction in system performance.

As the volume fraction increased to 45% and 50%, an interesting pattern emerged: As the non-relative pressure drop still followed the curve of the other volume fractions, the relative pressure drop actually decreased compared to the volume fraction at 40% (see Figure 4.1 (b)). This counter-intuitive behavior raises several possibilities that deserve consideration. Firstly, the unexpected reduction in pressure drop at higher hydrate volume fractions could be due to potential contamination within the system. Such contaminants could alter flow characteristics in ways that are not accounted for. The findings of Kvamme et al. [45] indicate that the presence of higher concentrations of hydrate particles in the presence of shear stress leads to more significant interactions with rusty surfaces. These interactions are characterised by increased mechanical impact and enhanced adsorption dynamics, both of which contribute to faster and more extensive rust formation.

Another plausible explanation is the incomplete conversion of cyclopentane to cyclopentane hydrates. If the conversion is not complete, the fluid dynamics within the system could be significantly different from what would be expected with a higher volume fraction of solid hydrate particles due to the presence of the third phase. However, specific checks for cyclopentane bubbles, which could indicate either unconverted cyclopentane or hydrates that have

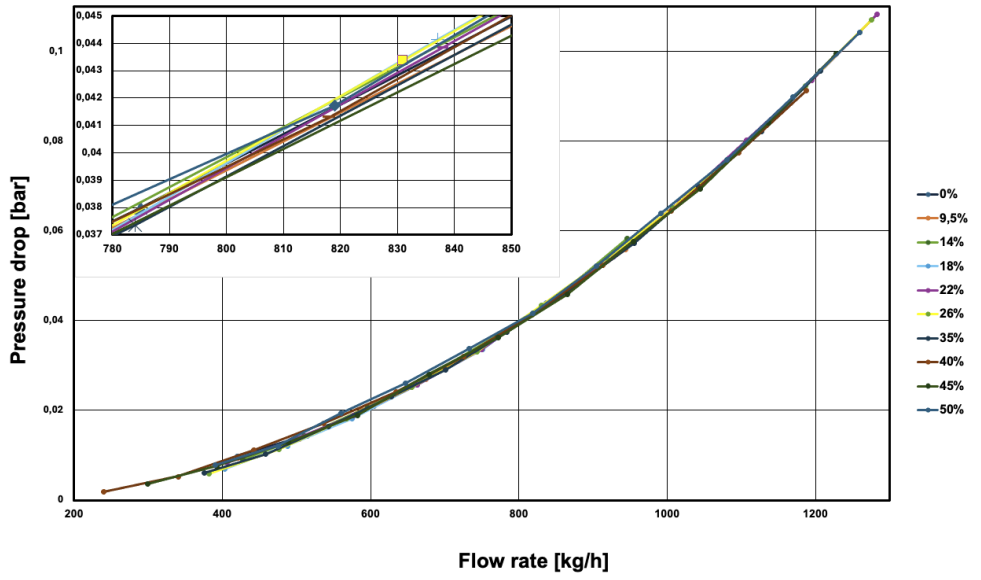

(a)

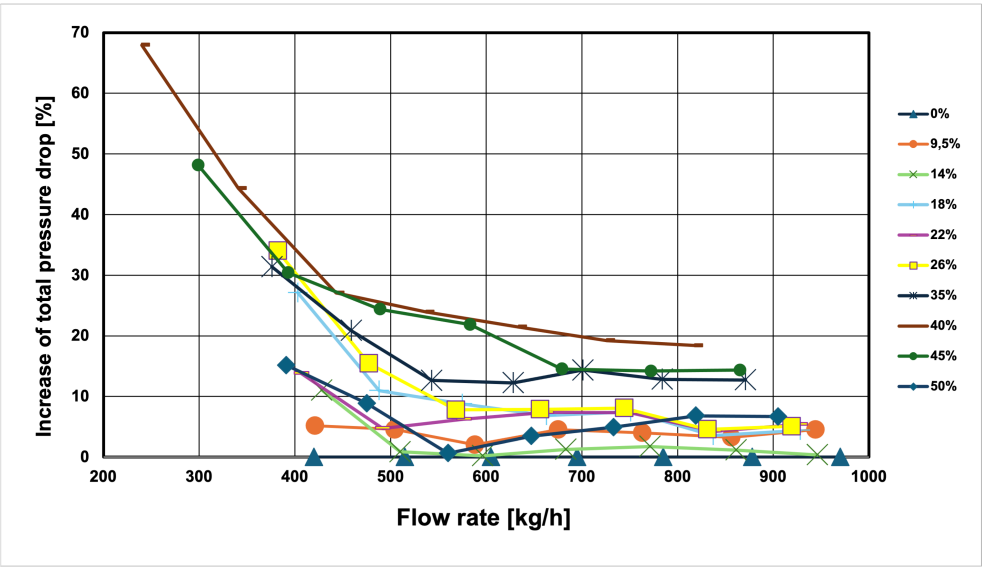

(b)

Figure 4.1: (a) Total pressure drop across the system, featuring an inset of a detailed, zoomed-in view for clearer observation, and (b) Relative increase in pressure drop compared to the baseline pressure drop observed with pure water. The percentages displayed represent various hydrate volume fractions within the system.

dissociated back into their constituents, showed no evidence of such events. Temperature measurements did not reveal any anomalies that would indicate unusual thermal activity or dissociation processes within the system.

This suggests that while the presence of hydrates generally increases pressure drop and reduces flow efficiency, complex interactions at higher volume fractions, possibly involving changes in the physical properties of the hydrate mixture or flow dynamics, may result in reduced impedance. This anomaly highlights the need for further investigation of the rheological properties of hydrate-rich flows and the effect of various factors such as purity, system fouling, and conversion efficiency on flow characteristics.

Overall, the results underscore the importance of considering both hydrate volume fraction and flow velocity in optimizing flow conditions and system performance. By elucidating the complex relationship between these parameters and pressure drop, the findings provide valuable guidance for the design and operation of flow systems involving cyclopentane hydrate slurries in water.

4.2 Blockage

In the investigation of blockage formation, the experimental setup was aimed at causing hydrate formation and subsequent plugging in the test section. Initial observations did not show immediate blockages, suggesting that cyclopentane hydrates do not create very cohesive particles. Subsequent experiments involved adjustments in operating parameters, including the introduction of additional cyclopentane to increase hydrate volume fraction. At volume fractions of 16 vol%, 18 vol%, 26 vol% and 35 vol%, no significant blockages were observed in the flow containing hydrate slurry close to the orifice.

However, at a volume fraction of 40%, a gradual decrease in the flow rate from around 80 kg/h to zero was observed within 40 minutes (see Figure 4.2). Figure 4.2 also illustrates how the temperature in the tank and in the test section diverged. This is an indication of hydrate accumulation around the temperature sensor, as the accumulations do not circulate with the rest of the slurry. As a result, these accumulations are more exposed to the higher temperatures from outside the pipe walls. The reduction in flow velocity indicated a significant obstruction to fluid movement. Further investigation revealed that blockages occurred from an initial flow rate of 135 kg/h, highlighting the critical influence of hydrate volume fraction on flow behavior and the occurrence of blockages. In general, the results emphasize the complex nature of hydrate behavior in pipeline systems and underscore the importance of considering volume fraction of hydrates in evaluating the blockage formation potential.

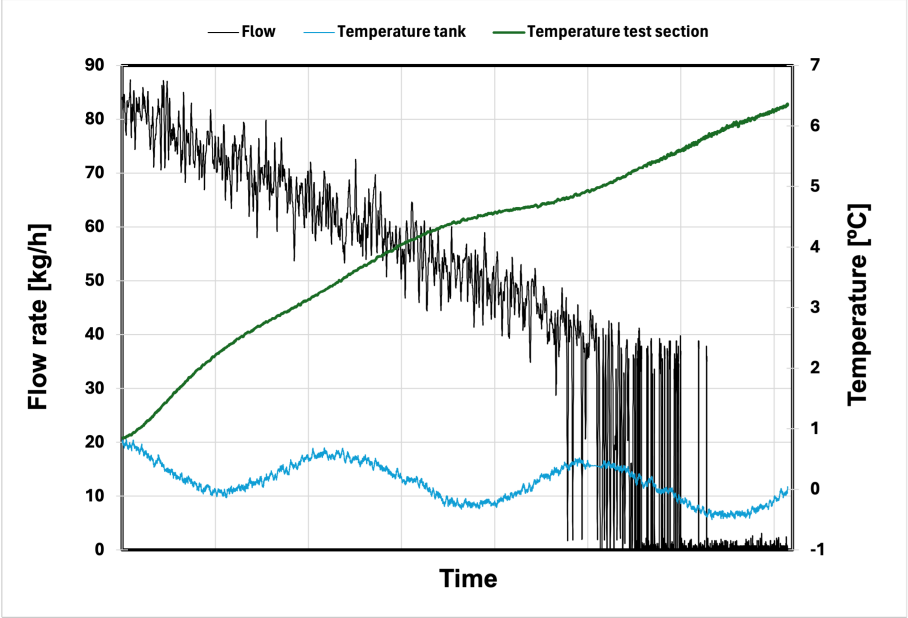

Figure 4.2: Flow decline until pipe blockage

When the volume fraction was further increased to 45% and 50%, there was no noticeable change compared to behavior observed at 40%, where blockage began to form from an initial flow rate of around 138 kg/h. This finding is intriguing as it may suggest that once a critical volume fraction threshold is reached, further increases in volume fraction do not necessarily exacerbate blockage severity. This could mean that the system reaches a saturation point where the physical layout or flow dynamics limit further accumulation of hydrates in a way that would increase blockage.

A clear pattern emerges at the volume fraction of 40% where a significant decrease in flow rate was observed, illustrating a boundary beyond which blockage is more likely to occur. The experimental data, and the diverging temperatures in the tank and test section as shown in Figure 4.2, support this observation. The isolation effect caused by the accumulation of hydrate around the temperature sensor at this volume fraction highlights the physical manifestation of blockages within the pipeline. As can be seen in Figure 3.4, the temperature sensor is in a 90° blind T-junction, so there may be accumulations in other corners in the flow loop that remain unidentified because sensors are not present.

This scenario highlights the critical influence of hydrates on the flow behavior within pipeline systems. It suggests that there is a critical volume fraction, observed here at 40%, above which the risk of blockage increases significantly. These results have important implications for pipeline operation and

management, emphasising the need to closely monitor and control hydrate volume fractions to prevent operational disruptions. Understanding and predicting the volume fraction at which hydrates begin to pose a serious risk of blockage is essential to develop effective strategies to mitigate these challenges in hydrate-prone pipeline systems.

Factors Influencing the Blockage Formation

The interaction between hydrate particles and pipeline materials is a key factor in understanding and managing the formation of blockages in fluid transport systems. Research indicates that the adhesive forces between cyclopentane hydrates and carbon steel are weaker than those between ice or other hydrates and carbon steel [7]. This reduced adhesion means that cyclopentane hydrates are less likely to adhere to pipeline walls, reducing the risk of blockage and making them particularly advantageous in practical applications where minimising disruption is critical.

Flow rate and turbulence also have an effect on the behavior of hydrate particles in pipelines. Higher flow rates can increase turbulence which can either be helping to keep hydrate particles suspended in the fluid and reducing the risk of blockage or lead to irregular growth patterns of hydrate particles, potentially increasing the likelihood of plug formation. Conversely, lower flow rates can lead to more laminar flow, allowing hydrates to settle or adhere, increasing the risk of blockage. Balancing flow rates to prevent hydrate aggregation without inducing excessive turbulence is therefore critical to effectively managing hydrate behavior.

To manage these risks, strategies such as applying non-stick coatings inside pipelines, optimising flow management and introducing chemical additives that alter hydrate surface properties can be effective. These measures will help to maintain operational efficiency and prevent the formation of blockages, ensuring smoother operation involving hydrate-prone pipeline systems. Future developments in technology and ongoing research will continue to refine these strategies and improve the reliability and safety of transporting fluids in various industrial contexts.

4.3 Uncertainties and Sources of Error

When conducting experiments in a flow loop system with water and cyclopentane hydrates, it is crucial to identify and address potential sources of error that may affect the accuracy and validity of the results. This section examines various uncertainties and their potential impact on experimental results. From

the accuracy of volume measurements to the consistency of chemical processes and the integrity of data acquisition systems, each source of error has the potential to significantly bias results. Understanding these factors is essential for the accurate interpretation of experimental data and the refinement of future research methodologies.

Measurement Accuracy

One source of uncertainty arises from the measurement of the volume of water added to the flow loop. This is done by weighing a container of water before and after it is emptied into the system. The accuracy of the scale used is uncertain, as any calibration error or environmental factors affecting the scale could cause deviations in the recorded weight. Similarly, measuring cyclopentane using a graduated cylinder could be subject to error. Graduated cylinders are prone to manufacturing inconsistencies that could affect the accuracy of the volume markings. In addition, the human element of reading the measurements introduces subjective variability, which could lead to further inaccuracies.

Instrumental and Data Acquisition Errors

In experimental settings, especially those involving complex systems such as flow loops, the accuracy of measuring instruments is critical. Even small variations can lead to significant deviations in data interpretation and results, see Table 3.1 for instrumental uncertainty. For example, variations between flow rates displayed on the flow meter and those recorded by the LabVIEW software are a good illustration on the challenges. The results shown on the flow meter were consistently lower by 5-30 kg/h can indicate errors in either the calibration of the flow meter, its accuracy, or the processing of the sensor signals by the data acquisition system. Another hypothesis is that the averaging time intervals might differ for the built-in controller and LabVIEW. In addition, temperature variations within the system caused by the varying power output of the chiller could affect reaction rates and hydrate stability. The inability of the chiller to maintain a constant temperature, as visible in tab 4.2 by the tank temperature, could introduce variability into the experimental conditions, affecting the reproducibility and reliability of the results.

Conversion and Dissociation

Another significant source of error could be the conversion of cyclopentane to hydrates and their stability in the experimental set-up. It is uncertain whether all the cyclopentane was completely converted into hydrates. Furthermore, these hydrates may have partially dissolved back into the solution during the course of the experiments, altering the expected results.

Rust and Contamination

The discovery of rust in the system represents a significant risk of contamination. Despite thorough cleaning and treatment of the immediate source of rust, residual contamination or other unknown sources could still affect the chemical reactions and integrity of the system (including possible abrasion of control elements). In addition, unanticipated contamination through openings in the tank could introduce additional variables not accounted for in the experimental design. Rusty surfaces inside pipelines can act as a catalyst for hydrate formation by adsorbing water molecules from the gas stream. When these water molecules bind to the rusty surfaces, a very thin layer of water is formed. Hydrate formation can then occur just outside this thin layer of water and can start immediately at the boundary of the adsorbed water layer [46].

Chapter 5

Conclusions and Suggestions for Further Work

The primary objective of this work was to investigate the flow behavior in a system containing cyclopentane hydrates at various volume fractions, with a particular focus on identifying hydrate volume fractions that pose a greater risk of plugging. To achieve this, a method was developed to generate cyclopentane hydrates in a dynamic system, specifically by constructing a flow loop.

The investigation of the pressure drop across the system was a key aspect of this study. Measurements were taken at volume fractions of hydrates ranging from 9.5% to 50%. This comprehensive investigation was critical to understanding how different volume fractions affected the hydraulic characteristics of the system and showed how pressure drop varied with increasing hydrate presence. The results demonstrated that higher volume fractions significantly affected the pressure dynamics within the flow loop, contributing to our understanding of hydrate behavior under varying flow conditions.

Following the pressure drop analysis, the study focused on investigating the formation of blockages. Blockages were studied at volume fractions ranging from 14% to 50%, with blockages first observed at 40%. The critical flow rate for blockage formation was approximately 135-140 kg/h, corresponding to a Reynolds number of approximately 2200. This finding was significant because it identified a specific critical volume fraction of hydrates above which the risk of blockage increased, providing valuable insights for pipeline management in hydrate-prone environments. Notably, these results contrast with previous studies of plug formation. Kilinc [13] observed plug formation at much higher hydrate volume fractions of 67% and 87% using cyclopentane hydrates. Struchalin and Balakin [10] utilized ice slurry in decane and observed blockages at volume fractions varying from 2.2 to 14%. These comparative observations underscore the complex nature of hydrate-related blockages and

highlight the necessity of tailoring blockage management strategies to specific hydrate systems and operating conditions in order to effectively mitigate risks in different industrial settings.

The observations indicated that cyclopentane hydrates are not highly cohesive, suggesting that they may be highly suitable for practical applications where a lower risk of clogging is beneficial, such as in the refrigeration processes of the fishing industry. This non-cohesiveness of cyclopentane hydrates could potentially make them suitable as a refrigerant, offering less risk of forming blockages that could disrupt system operation. Building on the basic knowledge presented, it is clear that Cyclopentane Hydrate Based Refrigeration Systems (HBRS) offers not just an alternative but a potentially revolutionary approach to refrigeration. The higher coefficient of performance (COP) of HBRS, as detailed in the studies, indicates a profound efficiency that could redefine energy consumption norms in cooling technologies. This efficiency not only contributes to lower operating costs, but also meets global environmental goals by minimising the carbon footprint of refrigeration systems. In addition, the use of cyclopentane hydrates, which operate effectively at lower pressures, improves safety and reduces the complexity and cost associated with the high-pressure systems traditionally used in refrigeration.

Experimental results obtained in this study allow us to conclude that HBRS solutions offer exciting advantages for a number of industrial and commercial sectors due to their scalability and ease of integration into existing technologies. The technology's adaptability to different cooling requirements, coupled with ongoing advances in system design and materials science, could see HBRS become more widespread. Particularly in industries where cooling is critical but the environmental and economic costs of conventional systems are increasingly unsustainable, HBRS could offer a sustainable and economically viable solution. Ongoing research and development, supported by empirical data from real-world applications, will be critical to overcoming any technical challenges and establishing HBRS as a standard in future refrigeration technologies. This approach not only promises improved cooling solutions, but also contributes to wider sustainability initiatives that are vital for future generations.

Building on the insights from this study, the application of Hydrate-Based Refrigeration Systems (HBRS) employing cyclopentane hydrates may represent a compelling solution for industries such as the fishing sector, where maintaining the quality of perishable goods through efficient and environmentally friendly cooling is of critical importance. Cyclopentane hydrates, with their lower cohesion and reduced risk of clogging, align well with the needs of onboard refrigeration systems that aim to minimize the enzymatic and bacteriological degradation of fish. Furthermore, the thermodynamic properties of

cyclopentane hydrates contribute to their suitability for such applications. They exhibit high efficiency in thermal energy storage and transfer, which makes them particularly effective for maintaining consistent cooling over extended periods. Moreover, cyclopentane hydrates are stable at relatively low pressures compared to other types of hydrates, which translates to safer and more cost-effective operating conditions. These characteristics not only enhance the practicality of cyclopentane hydrates in refrigeration applications but also bolster their potential to improve sustainability and operational efficiency in the fishing industry and beyond.

Suggestions for Further Work

Further research is necessary to address remaining questions regarding the behavior and applications of cyclopentane hydrates. The formation and management of hydrates in pipeline systems presents complex challenges, and ongoing research is essential to deepen our understanding and improve operational strategies. An important area for further work is to replicate the experiments conducted in this study under similar conditions to confirm the findings. Reproducibility is essential to establish reliable data and validate the observed behaviors and results. By conducting these experiments multiple times, researchers can ensure that the results are reliable and not anomalous, thereby solidifying the conclusions drawn about hydrate formation and plugging potential at different volume fractions.

Furthermore, there is a need to investigate the thermodynamic properties of cyclopentane hydrates to evaluate their potential use as refrigerants. This involves a series of experiments designed to measure various thermodynamic variables under controlled conditions. The objective is to provide insight into the energy efficiency, cooling capacity and environmental impact of using cyclopentane hydrates in refrigeration systems. Understanding these properties could open up new avenues for the application of hydrates in refrigeration technologies, particularly in sectors where non-toxic and non-flammable refrigerants are required.

Further experiments should also be carried out to prepare emulsion samples under conditions more favorable for hydrate formation, in order to thoroughly investigate the prerequisites for hydrate formation under static conditions. These experiments would help to identify the exact environmental and chemical conditions that favour the formation of stable hydrates. By adjusting variables such as temperature and pressure, researchers can develop a clearer

understanding of how cyclopentane hydrates behave in different environments and what could be done to promote or inhibit their formation.

The formation of rust particles within a flowing system has been observed to act as ”seed sites” for heterogeneous nucleation, thereby enhancing nucleation rates and promoting crystallisation. It is therefore proposed that an experimental setup intended to be overhauled soon to be utilised to conduct flow loop experiments, with the objective of reproducing and studying likely industrial scenarios of metal parts rubbing against each other and creating rust particles, which will subsequently enter the flow and affect its behavior.

Through these suggested areas of further work, we aim not only to confirm the findings of this thesis, but also to expand the knowledge surrounding cyclopentane hydrates, facilitating their safer and more effective use in industry.

Bibliography

[1] E. D. Sloan. Jr. and C. Koh. *Clathrate Hydrates of Natural Gases.* Chemical industries/119. CRC Press, 2007. ISBN 978-1-4200-0849-4.

[2] Kristina Norne Widell, Eirik Starheim Svendsen, and Tom Ståle Nordtvedt. Possibilites of ice slurry systems onboard fishing vessels. *Ammonia & CO2 Refrigeration Technologies*, 2023.

[3] Wenxiang Zhang, Yanhong Wang, Xuemei Lang, and Shuanshi Fan. Performance analysis of hydrate-based refrigeration system. *Energy Conversion and Management*, 146:43–51, 2017. ISSN 0196-8904. doi: https://doi.org/10.1016/j.enconman.2017.04.091. URL `https://www.sciencedirect.com/science/article/pii/S0196890417304120`.

[4] Flemming Jessen, Jette Nielsen, and Erling Larsen. *Seafood Processing: Technology, Quality and Safety*, chapter 3. Chilling and Freezing of Fish. John Wiley and Sons, Incorporatedy, 2014.

[5] Henry Delroisse, Jean-Philippe Torré, and Christophe Dicharry. Effect of a hydrophilic cationic surfactant on cyclopentane hydrate crystal growth at the water/cyclopentane interface. *Crystal Growth & Design*, 17(10): 5098–5107, 2017. doi: 10.1021/acs.cgd.7b00241.

[6] Masahiro Nakajima, Ryo Ohmura, and Yasuhiko H. Mori. Clathrate hydrate formation from cyclopentane-in-water emulsions. *Industrial & Engineering Chemistry Research*, 47(22):8933–8939, 2008. doi: 10.1021/ie800949k.

[7] Joseph W. Nicholas, Laura E. Dieker, E. Dendy Sloan, and Carolyn A. Koh. Assessing the feasibility of hydrate deposition on pipeline walls—adhesion force measurements of clathrate hydrate particles on carbon steel. *Journal of Colloid and Interface Science*, 331(2):322–328, 2009. ISSN 0021-9797. doi: https://doi.org/10.1016/j.jcis.2008.11.070. URL `https://www.sciencedirect.com/science/article/pii/S0021979708015919`.

[8] Zachary M Aman, Sanjeev E Joshi, E Dendy Sloan, Amadeu K Sum, and Carolyn A Koh. Micromechanical cohesion force measurements to determine cyclopentane hydrate interfacial properties. *Journal of colloid and interface science*, 376(1):283–288, 2012.

[9] Pavel G Struchalin, Vegar H Øye, Pawel Kosinski, Alex C Hoffmann, and Boris V Balakin. Flow loop study of a cold and cohesive slurry. pressure drop and formation of plugs. *Fuel*, 332:126061, 2023.

[10] Pavel G Struchalin and Boris V Balakin. Blocking dead zones to avoid plugs in pipes. *Chemical Engineering Research and Design*, 194:649–652, 2023.

[11] Boris V. Balakin, Yu-Fen Chang, Mona Øynes, and Pavel G. Struchalin. Plugging of pipes by cohesive particles. computed tomography investigation and theoretical analysis. *Chemical Engineering Science*, 296:120214, 2024. ISSN 0009-2509. doi: https://doi.org/10.1016/j.ces.2024.120214. URL `https://www.sciencedirect.com/science/article/pii/S0009250924005141`.

[12] Madina Naukanova, Gianluca Lavalle, Jean-Michel Herri, Ana Cameirao, Pavel G Struchalin, and Boris V Balakin. Viscosity of ice-in-oil slurries. *International Journal of Refrigeration*, 150:41–46, 2023.

[13] Z Kilinc. Formation and particle size distribution of cyclopentane hydrates in a multiphase flow system, 2008.

[14] E Dendy Sloan. Clathrate hydrates: the other common solid water phase. *Industrial & Engineering Chemistry Research*, 39(9):3123–3129, 2000.

[15] Peter Englezos. Clathrate hydrates. *Industrial & engineering chemistry research*, 32(7):1251–1274, 1993.

[16] E. Dendy Sloan. Clathrate hydrates: The other common solid water phase. *Ind. Eng. Chem. Res.*, 39(9):3123–3129, 2000. doi: 10.1021/ie000574c.

[17] Charles W Beckett, Kenneth S Pitzer, and Ralph Spitzer. The thermodynamic properties and molecular structure of cyclohexane, methylcyclohexane, ethylcyclohexane and the seven dimethylcyclohexanes1. *Journal of the American Chemical Society*, 69(10):2488–2495, 1947.

[18] Robert A Pierotti and Albert A Liabastre. The structure and properties of water solutions. 1972.

[19] Joonseop Lee, Young Keun Jin, and Yongwon Seo. Characterization of cyclopentane clathrates with gaseous guests for gas storage and separation. *Chemical Engineering Journal*, 338:572–578, 2018. ISSN 1385-8947. doi: https://doi.org/10.1016/j.cej.2018.01.054. URL https://www.sciencedirect.com/science/article/pii/S1385894718300706.

[20] Pramod Warrier, M. Naveed Khan, Vishal Srivastava, C. Mark Maupin, and Carolyn A. Koh. Overview: Nucleation of clathrate hydrates. *The Journal of Chemical Physics*, 145(21):211705, 2016. doi: 10.1063/1.4968590.

[21] Qiunan Lv and Xiaosen Li. Raman spectroscopic studies on microscopic mechanism of cp - ch4 mixture hydrate. *Energy Procedia*, 142:3264–3269, 2017. ISSN 1876-6102. doi: https://doi.org/10.1016/j.egypro.2017.12.501. URL https://www.sciencedirect.com/science/article/pii/S1876610217362562. Proceedings of the 9th International Conference on Applied Energy.

[22] Mostafa Abolala and Farshad Varaminian. Thermodynamic model for predicting equilibrium conditions of clathrate hydrates of noble gases+light hydrocarbons: Combination of van der waals–platteeuw model and spc-saft eos. *The Journal of Chemical Thermodynamics*, 81:89–94, 2015. ISSN 0021-9614. doi: https://doi.org/10.1016/j.jct.2014.09.013. URL https://www.sciencedirect.com/science/article/pii/S0021961414002985.

[23] Bjorn Kvamme and Hideki Tanaka. Thermodynamic stability of hydrates for ethane, ethylene, and carbon dioxide. *The Journal of Physical Chemistry*, 99(18):7114–7119, 1995.

[24] Erika Brown, M. Naveed Khan, Davi Salmin, Jonathan Wells, Shenglong Wang, Cornelis J. Peters, and Carolyn A. Koh. Cyclopentane hydrate cohesion measurements and phase equilibrium predictions. *Journal of Natural Gas Science and Engineering*, 35:1435–1440, 2016. ISSN 1875-5100. doi: https://doi.org/10.1016/j.jngse.2016.05.016. URL https://www.sciencedirect.com/science/article/pii/S1875510016303158. Gas Hydrates and Applications.

[25] Ragnhild B Asserson, Alex C Hoffmann, Sylvi Høiland, and Kjell M Asvik. Interfacial tension measurement of freon hydrates by droplet deposition and contact angle measurements. *Journal of Petroleum Science and Engineering*, 68(3-4):209–217, 2009.

[26] Zachary M. Aman et al. Surfactant adsorption and interfacial tension investigations on cyclopentane hydrate. *Langmuir*, 2013.

[27] Jorge Benet, Luis G MacDowell, and Eduardo Sanz. A study of the ice–water interface using the tip4p/2005 water model. *Physical Chemistry Chemical Physics*, 16(40):22159–22166, 2014.

[28] Soumi Banerjee, Eveline Hassenklöver, J. Mieke Kleijn, Martien A. Cohen Stuart, and Frans A. M. Leermakers. Interfacial tension and wettability in water–carbon dioxide systems: Experiments and self-consistent field modeling. *The Journal of Physical Chemistry B*, 117(28):8524–8535, 2013. doi: 10.1021/jp400940s.

[29] Carlos Drummond and Jacob Israelachvili. Surface forces and wettability. *Journal of Petroleum Science and Engineering*, 33(1):123–133, 2002. ISSN 0920-4105. doi: https://doi.org/10.1016/S0920-4105(01)00180-2. URL `https://www.sciencedirect.com/science/article/pii/S0920410501001802`. Evaluation of reservoir wettability.

[30] Tomohiro Ogawa, Tomonari Ito, Kenji Watanabe, Ken-ichi Tahara, Ryuzo Hiraoka, Jun-ichi Ochiai, Ryo Ohmura, and Yasuhiko H Mori. Development of a novel hydrate-based refrigeration system: A preliminary overview. *Applied thermal engineering*, 26(17-18):2157–2167, 2006.

[31] Nan Xie, Chenghua Tan, Sheng Yang, and Zhiqiang Liu. Conceptual design and analysis of a novel co2 hydrate-based refrigeration system with cold energy storage. *ACS Sustainable Chemistry & Engineering*, 7 (1):1502–1511, 2019. doi: 10.1021/acssuschemeng.8b05255.

[32] Department of Climate Change Energy the Environment and Water. Ozone protection and synthetic greenhouse gas management act 1989, 2023. URL `https://www.legislation.gov.au/C2004A03755/latest/text`. Accessed: 28.05.2024.

[33] Pijush K. Kundu, Ira M. Cohen, and David R. Dowling. *Fluid Mechanichs*. Elsevier Science, sixth edition, 2016.

[34] Frank M. White and Henry Xue. *Fluid Mechanics*. McGraw Hill LLC, ninth edition, 2021.

[35] Masoumeh Akhfash, John A Boxall, Zachary M Aman, Michael L Johns, and Eric F May. Hydrate formation and particle distributions in gas–water systems. *Chemical Engineering Science*, 104:177–188, 2013.

[36] Zachary M Aman, Erika P Brown, E Dendy Sloan, Amadeu K Sum, and Carolyn A Koh. Interfacial mechanisms governing cyclopentane clathrate hydrate adhesion/cohesion. *Physical Chemistry Chemical Physics*, 13 (44):19796–19806, 2011.

[37] Zachary M. Aman, William J. Leith, Giovanny A. Grasso, E. Dendy Sloan, Amadeu K. Sum, and Carolyn A. Koh. Adhesion force between cyclopentane hydrate and mineral surfaces. *Langmuir*, 29(50):15551–15557, 2013. doi: 10.1021/la403489q. PMID: 24266729.

[38] G. Aspenes, L.E. Dieker, Z.M. Aman, S. Høiland, A.K. Sum, C.A. Koh, and E.D. Sloan. Adhesion force between cyclopentane hydrates and solid surface materials. *Journal of Colloid and Interface Science*, 343 (2):529–536, 2010. ISSN 0021-9797. doi: https://doi.org/10.1016/j.jcis.2009.11.071. URL https://www.sciencedirect.com/science/article/pii/S0021979709015367.

[39] CJ Taylor. Pole assignment control of state dependent parameter models: further examples and generalisations. Technical report, Technical Report, Engineering Department, Lancaster University, UK, 2005.

[40] Astrid Döppenschmidt and Hans-Jürgen Butt. Measuring the thickness of the liquid-like layer on ice surfaces with atomic force microscopy. *Langmuir*, 16(16):6709–6714, 2000.

[41] Sijia Hu and Carolyn A. Koh. Interfacial properties and mechanisms dominating gas hydrate cohesion and adhesion in liquid and vapor hydrocarbon phases. *Langmuir*, 33(42):11299–11309, 2017. doi: 10.1021/acs.langmuir.7b02676.

[42] Shenglong Wang, Shuanshi Fan, Xuemei Lang, Yanhong Wang, and Pengfei Wang. Particle size dependence of clathrate hydrate particle cohesion in liquid/gaseous hydrocarbons. *Fuel*, 259:116201, 2020. ISSN 0016-2361. doi: https://doi.org/10.1016/j.fuel.2019.116201. URL https://www.sciencedirect.com/science/article/pii/S0016236119315558.

[43] Son Ho-Van, Baptiste Bouillot, Daniel Garcia, Jérome Douzet, Ana Cameirao, Saheb Maghsoodloo-Babakhani, and Jean-Michel Herri. Crystallization mechanisms and rates of cyclopentane hydrates formation in brine. *Chemical engineering & technology*, 42(7):1481–1491, 2019.

[44] Keitatsu Kamochi, Ayushman Tripathi, Masanao Taoka, Ryo Ohmura, and Keita Yasuda. Phase equilibrium conditions in cyclopentane hydrate forming systems coexisting with sodium chloride aqueous solution under atmospheric pressure and vacuum condition. *The Journal of Chemical Thermodynamics*, 175:106886, 2022. ISSN 0021-9614. doi: https://doi.org/10.1016/j.jct.2022.106886. URL https://www.sciencedirect.com/science/article/pii/S0021961422001653.

[45] Bjørn Kvamme, Solomon Aforkoghene Aromada, Navid Saeidi, Thomas Hustache-Marmou, and Petter Gjerstad. Hydrate nucleation, growth, and induction. *ACS Omega*, 5(6):2603–2619, 2020. doi: 10.1021/acsomega.9b02865. PMID: 32095684.

[46] Bjørn Kvamme and Solomon Aforkoghene Aromada. Alternative routes to hydrate formation during processing and transport of natural gas with a significant amount of co2: Sleipner gas as a case study. *Journal of Chemical & Engineering Data*, 63(3):832–844, 2018. doi: 10.1021/acs.jced.7b00983.

Appendix A

LabVIEW script

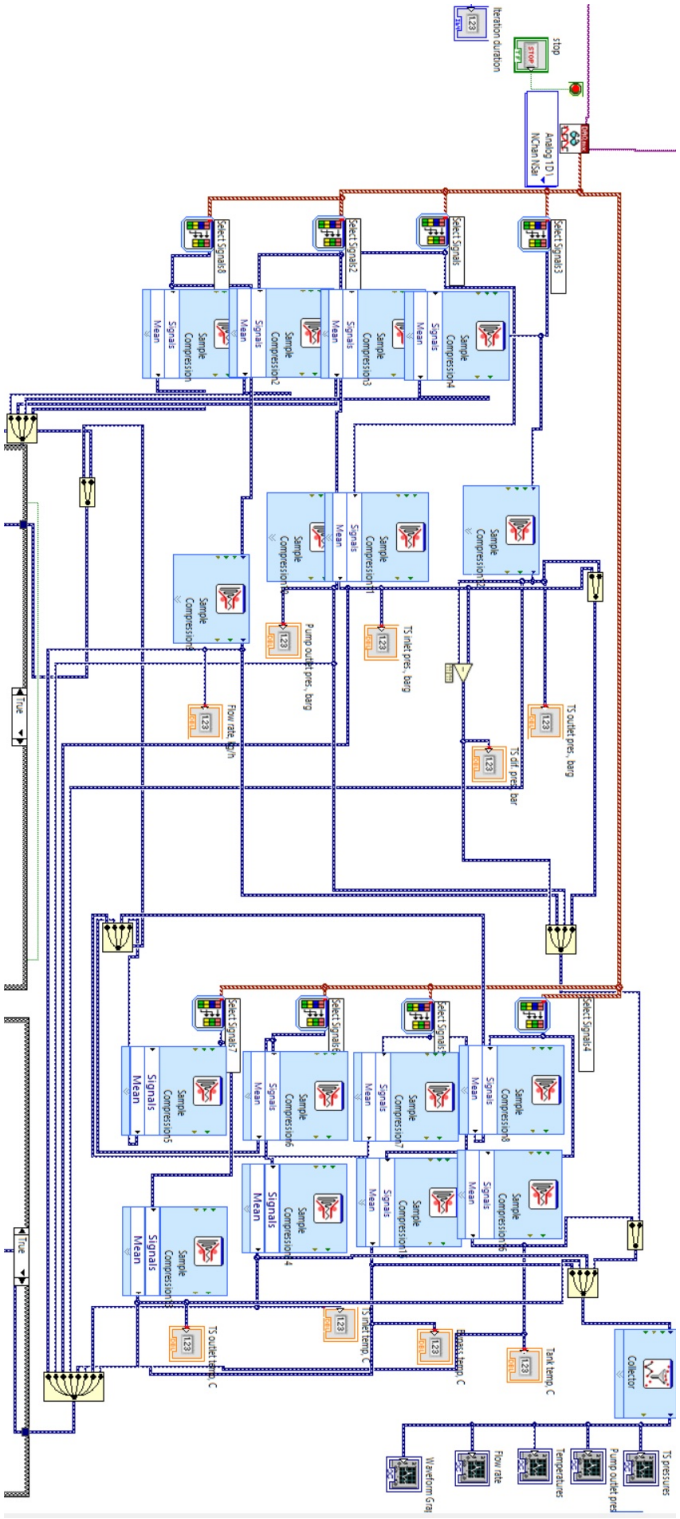
Iteration duration
stop
Analog 1D
Select Signals8
Select Signals2
Select Signals1
Select Signals3
Sample Compression4
Sample Compression3
Sample Compression2
Sample Compression
Signals
Mean
Pump outlet pres. barg
TS inlet pres. barg
Flow rate kg/h
TS outlet pres. barg
TS set pres. bar
Select Signals7
Select Signals5
Select Signals6
Select Signals4
Sample Compression7
Sample Compression6
Sample Compression5
Sample Compression8
TS outlet temp C
TS inlet temp C
Basin temp C
Tank temp C
Collector
Waveform Graph
Flow rate
Temperatures
Pump outlet pres
TS pressures

Appendix B

Calculations for amount of cyclopentane to be added

The concept of ”number of moles” quantifies the amount of substance present in a given sample, typically measured in moles. One mole of a substance makes $6.022 \cdot 10^{23}$ number of constituent particles of that substance. To make one mole of cyclopentane hydrate, there needs to be 136 moles of water molecules and 8 cyclopentane molecules. The number of moles of hydrates is determined by the following equation.

$$n_{\text{hyd}} = \frac{V_{\text{hyd}} \cdot \rho_{\text{hyd}}}{Mm_{\text{hyd}}} \tag{B.1}$$

The volume of cyclopentane can be defined through the number of moles and the density of the liquid.

$$V_{\text{cp}} = \frac{n_{\text{cp}} \cdot Mm_{\text{cp}}}{\rho_{\text{cp}}} \tag{B.2}$$

Based on Equation (3.1) n_{cp} can be replaced by $n_{w,\ hyd}$ divided by 17.

$$V_{\text{cp}} = \frac{n_{\text{w, hyd}} \cdot Mm_{\text{cp}}}{17 \cdot \rho_{\text{cp}}} \tag{B.3}$$

The mass of the hydrates in the system can be written as

$$m_{\text{hyd}} = n_{\text{cp}} \cdot Mm_{\text{cp}} + n_{\text{w, hyd}} \cdot Mm_{\text{w, hyd}} \tag{B.4}$$

As calculated in Equation (B.3), based on (3.1), n_{cp} is replaced.

$$m_{\text{hyd}} = \frac{n_{\text{w, hyd}} \cdot Mm_{\text{cp}}}{17} + n_{\text{w, hyd}} \cdot Mm_{\text{w}} = n_{\text{w, hyd}}(\frac{Mm_{\text{cp}}}{17} + Mm_{\text{w}}) \tag{B.5}$$

The number of moles can be defined by its mass divided by its molar mass. Then, using (B.5) and replacing m_{hyd}, we get

$$n_{\text{hyd}} = \frac{m_{\text{hyd}}}{Mm_{\text{hyd}}} = \frac{n_{\text{w, hyd}}(\frac{Mm_{\text{cp}}}{17} + Mm_{\text{w}})}{Mm_{\text{hyd}}} \tag{B.6}$$

Isolating $n_{\text{w, hyd}}$ gives the following equation.

$$n_{\text{w, hyd}} = \frac{n_{\text{hyd}} \cdot Mm_{\text{hyd}}}{\frac{Mm_{\text{cp}}}{17} + Mm_{\text{w}}} \tag{B.7}$$

The total volume of the system compared to the volume occupied by the hydrates is defined as

$$V_{\text{tot}} = \frac{V_{\text{hyd}}}{C_{\text{hyd}}} \tag{B.8}$$

Using Equation (B.7) and replacing n_{hyd} based on Equation (B.1), Mm_{hyd} will cancel out and result in

$$n_{\text{w, hyd}} = \frac{V_{\text{hyd}} \cdot \rho_{\text{hyd}}}{\frac{Mm_{\text{cp}}}{17} + Mm_{\text{w}}} \tag{B.9}$$

And by replacing V_{hyd} by using Equation (B.8), we get the following equation.

$$n_{\text{w, hyd}} = \frac{C_{\text{hyd}} \cdot V_{\text{tot}} \cdot \rho_{\text{hyd}}}{\frac{Mm_{\text{cp}}}{17} + Mm_{\text{w}}} \tag{B.10}$$

After that V_{cp} is isolated, because we want to know how much cyclopentane is necessary to add to get a specific volume percentage of hydrates in the system. This is done by replacing $n_{\text{W, hyd}}$ in Equation (B.3) by implementing Equation (B.10). From that, we get

$$V_{\text{cp}} = \frac{Mm_{\text{cp}}}{17 \cdot \rho_{\text{cp}}} \cdot \frac{C_{\text{hyd}} \cdot V_{\text{tot}} \cdot \rho_{\text{hyd}}}{\frac{Mm_{\text{cp}}}{17} + Mm_{\text{w}}} \tag{B.11}$$

Which can be simplified into the final equation.

$$V_{\mathrm{cp}} = \frac{C_{\mathrm{hyd}} \cdot V_{\mathrm{tot}} \cdot Mm_{\mathrm{cp}} \cdot \rho_{\mathrm{hyd}}}{(Mm_{\mathrm{cp}} + 17 \cdot Mm_{\mathrm{w}}) \cdot \rho_{\mathrm{cp}}} \tag{B.12}$$

Equation B.12 depends on $\mathrm{V_{tot}}$ to calculate V_{cp}. This makes it not a fully independent equation, because V_{tot} is not a fixed value and varies depending on the value of V_{cp}. However, there is a simple solution to this problem. By iterating $\mathrm{V_{tot}}$ based on the latest result of $\mathrm{V_{cp}}$ three times, the difference between the iterations becomes less than 0.001 L.

To do the iterations, an assumptions that $\mathrm{V_{tot}}$ is the same volume as the amount of water which is added in the flow loop. By using Equation B.12 we obtain a volume of cyclopentane. With that volume, we need to find out how much the volume of the system would increase by after the hydrate formation from the cyclopentane. To calculate this, first find out the number of moles in the given volume of cyclopentane. Then calculate the volume of the formed hydrates with the following equation:

$$V_{\mathrm{hyd}} = \frac{n_{\mathrm{hyd}} \cdot Mm_{\mathrm{hyd}}}{\rho_{\mathrm{hyd}}} \tag{B.13}$$

Then, the volume of the liquid water already in the system that now forms hydrate cages needs to be subtracted from the total volume of the system while the volume of the hydrates is added. The increase in volume of the system is calculated from the following equation:

$$V_{\mathrm{tot,\,i+1}} - V_{\mathrm{tot,\,i}} = V_{\mathrm{hyd,\,i}} - \frac{136 \cdot n_{\mathrm{hyd,\,i}} \cdot Mm_{\mathrm{w}}}{\rho_{\mathrm{w}}} \tag{B.14}$$

After calculating the increase of the total volume of the system, add the increase to $\mathrm{V_{tot}}$ in Equation B.12. Then, a new value for $\mathrm{V_{cp}}$, will be derived to further iterate until the difference between the iterations satisfies the accuracy criteria.

For example, if the flow loop is filled with 28 litres of water and the desired volume fraction of hydrates is 14%, firstly we can use Equation B.12.

$$V_{\mathrm{cp}} = \frac{0.14 \cdot 0.028\,m^3 \cdot 70.1 \frac{kg}{kmol} \cdot 954 \frac{kg}{m^3}}{(70.1 \frac{kg}{kmol} + 17 \cdot 18.02 \frac{kg}{kmol}) \cdot 751 \frac{kg}{m^3}} = 927.3 \cdot 10^{-6}\,m^3 \tag{B.15}$$

Equation B.15 indicates the need to add approximately 0.93 liters of cyclopentane. However, with the addition of cyclopentane, the total volume, V_{tot},

undergoes a change, which makes the value used in Equation B.15 incorrect. To determine this change, assuming complete conversion of cyclopentane to hydrates, we use Equation B.13 to determine the volume of hydrates that is formed by 0,93 liters of cyclopentane. Initially, it is essential to calculate the number of moles of hydrates produced based on the volume of cyclopentane in the system. Given that the number of moles of hydrates is eight times less than that of cyclopentane, we calculate the number of moles of cyclopentane and then divide it by eight.

$$n_{\text{hyd}} = \frac{927.3 \cdot 10^{-6} m^3 \cdot 751 \frac{kg}{m^3}}{8 \cdot 70.1 \frac{kg}{kmol}} = 1.24 \cdot 10^{-3} kmol \tag{B.16}$$

As we now have the number of moles of hydrates from the calculated amount of cyclopentane, we're able to calculate the volume of this amount of hydrates.

$$V_{\text{hyd}} = \frac{1.24 \cdot 10^{-3} kmol \cdot (136 \cdot 18.02 + 8 \cdot 70.1) \frac{kg}{kmol}}{951 \frac{kg}{m^3}} = 3.93 \cdot 10^{-3} m^3 \tag{B.17}$$

Then, we use Equation B.14 to iterate to the actual necessary amount of cyclopentane to add to the system. This leads to the estimate of 0.957 liters of cyclopentane required to reach 14% hydrates in a system with 28 liters of water.